Chapter 2: SAC-CI Method: Theoretical Aspects and Some Recent Topics

Hiroshi Nakatsuji

Department of Synthetic Chemistry and Biological Chemistry

Faculty of Engineering, Kyoto University, Kyoto 606-01, Japan

and

Institute for Fundamental Chemistry

34-4 Takano-Nishihiraki-cho, Sakyo-ku, Kyoto 606, Japan

E-mail: hiroshi@synchem.kyoto-u.ac.jp

Abstract

Theoretical aspects of the SAC/SAC-CI method for calculating ground, excited, ionized, and electron attached states of molecules are summarized. The SAC-CI SD (singles and doubles) method for the ground and excited states of singlet to septet spin multiplicities and the SAC-CI general-*R* method for two-to-many electron excitation processes are described and their accuracies are explained based on the computed results. Some recent topics of interest in the applications such as the spectra of metal complexes, the collision induced absorption spectra of CsXe, and the excitation spectra of porphyrins are reviewed. The SAC/SAC-CI method is shown to be simple enough to be useful and accurate enough to be useful.

Contents

1. Electronic theory for excited states

What condition characterizes the excited states? Using the Schrödinger equation,

$$H\Psi_n = E_n\Psi_n \tag{1}$$

the excited state is characterized as the solution not having the lowest energy eigenvalue. When the system has no symmetry at all, this is the only one condition defining the excited state. Let us write the ground state wave function as Ψ_g and the excited one by Ψ_e, then they should satisfy

$$\langle\Psi_g|\Psi_e\rangle = 0, \tag{2a}$$

$$\langle\Psi_g|H|\Psi_e\rangle = 0. \tag{2b}$$

This is the condition that the ground and excited states must satisfy: otherwise the wave function is a mixture of the ground and excited states.

This argument implies that the theory for the excited states can not be independent of the theory for the ground state. Two theories should be designed to be consistent to each other and this consistency should be kept at any level of approximations up to the exact limit. The SAC/SAC-CI theory is such a theory. The SAC (symmetry adapted cluster) theory is the theory for the ground state[1,2] and the SAC-CI (configuration interaction) theory is the theory for the excited states.[3-7] As

always is, we mean by excited states not only the excited states, but also the ionized states and the electron attached states.

We give here a review on the theoretical aspects and on the recent applications of the SAC/SAC-CI method. Some reviews were already published;[8-13] general and on the computer code,[8,10,11] on the excited and ionized states of conjugated molecules,[9] on the applications to surface reactions,[12] and on the excited states of porphyrins.[13] The computer code was already published[14,15] and the more recent current version[16] is also available on request to the author.

2. Hartree-Fock and SECI theories as a warming-up

There is a beautiful theoretical relationship between the Hartree-Fock (HF) theory for the ground state and the single excitation (SE) CI theory for the excited states. It is analogous to the relationship between the SAC and SAC-CI theories. For the HF and SECI theories, the Brillouin theorem is a key theorem which interconnects these two theories. We consider, for a while, a closed-shell ground state with 2n electrons, and the excited and ionized states produced therefrom.

The HF molecular orbital theory is a good starting approximation for the ground state. It assumes a single determinant wave function,

$$\Psi_g^{HF} = \| \varphi_1\alpha\varphi_1\beta ... \varphi_i\alpha\varphi_i\beta ... \varphi_n\alpha\varphi_n\beta \| , \tag{3}$$

where molecular orbitals φ_i are the solutions of the Fock equation,

$$F\varphi_i = \varepsilon_i\varphi_i , \tag{4}$$

with ε_i being orbital energies. Generally speaking, the HF model is appropriate for molecules near equilibrium geometry.

We now introduce a singly excited configuration Φ_i^a given by

$$\Phi_i^a = \| \varphi_1\alpha\varphi_1\beta ... \varphi_i\varphi_a (\alpha\beta - \beta\alpha)/\sqrt{2} ... \varphi_n\alpha\varphi_n\beta \| . \tag{5}$$

Then, the HF wave function and the SECI configuration satisfy the Brillouin theorem,

$$\langle \Psi_g^{HF} | H | \Phi_i^a \rangle = 0, \tag{6a}$$

and the orthogonality,

$$\langle \Psi_g^{HF} | \Phi_i^a \rangle = 0 . \tag{6b}$$

It is easy to show that the Brillouin theorem is theoretically equivalent with the HF equation given by Eq. (4).

We note that the relation given by Eq. (6) is formally identical with Eq. (2). Therefore, Eq. (6) implies that if Ψ_g^{HF} is a good approximation of the ground state Ψ_g, the singly excited

configurations $\{\Phi_i^a\}$ may give a good basis for describing the excited states Ψ_e. Then, we expand the excited state by a linear combination of Φ_i^a, i.e.,

$$\Psi_e^{SECI} = \sum_{i,a} C_i^a \Phi_i^a , \tag{7}$$

which is the SECI method. The coefficients C_i^a are determined by projecting the Schrödinger equation onto the space of $\{\Phi_i^a\}$, i.e.,

$$\langle \Phi_i^a | H - E | \Psi_e^{SECI} \rangle = 0 , \tag{8}$$

which is a secular equation. The solutions automatically satisfy

$$\langle \Psi_g^{HF} | \Psi_e^{SECI} \rangle = 0 , \qquad \langle \Psi_g^{HF} | H | \Psi_e^{SECI} \rangle = 0 , \tag{9}$$

as a result of the Brillouin theorem. Different solutions of Eq. (8) satisfy

$$\langle \Psi_e^{SECI} | \Psi_f^{SECI} \rangle = 0 , \qquad \langle \Psi_e^{SECI} | H | \Psi_f^{SECI} \rangle = 0 . \tag{10}$$

Eq. (9) shows that the HF and SECI wave functions satisfy mutually correct relations as given by Eq. (2) so that we expect that the SECI method may describe the excited states as well as the HF method does the ground state.

Similar relations hold for ionized states and electron attached states. In the HF model, the ionization energy from the orbital φ_i is written by the Koopmans' relation as,

$$Ip(i) = -\varepsilon_i , \tag{11}$$

and the corresponding ionized state is written by

$$\Psi_i = \| \varphi_1 \alpha \varphi_1 \beta ... \varphi_i \alpha ... \varphi_n \alpha \varphi_n \beta \| . \tag{12}$$

It is easy to show the relations,

$$\langle \Psi_i | \Psi_g^{HF} \rangle = 0 , \qquad \langle \Psi_i | H | \Psi_g^{HF} \rangle = 0 , \tag{13}$$

and

$$\langle \Psi_i | \Psi_j \rangle = \delta_{ij} , \qquad \langle \Psi_i | H | \Psi_j \rangle = \delta_{ij} . \tag{14}$$

Eq. (13) corresponds to Eq. (6), and Eq. (14) means that the secular equation, Eq. (8) is already diagonal for the ionized configurations Ψ_i. Thus, the Koopmans' relation is valid up to SECI. Similar relations hold for electron attached states.

Theoretical simplicity of the HF/SECI theory is beautiful, but this does not necessarily mean that it gives quantitatively reliable results for the ground, excited, ionized, and electron attached states. Actually our experiences show that the SECI and Koopmans methods are not satisfactory for quantitative purposes: usually the agreement with experiment is poor when we use these methods. Thus, electron correlations are important for describing excitation and ionization properties.

We note that the theoretical consistency of the HF/SECI theory is valid only up to single excitations. The Brillouin theorem means that the first correction to the HF wave function is an inclusion of doubly excited configurations. When such configurations are included (e.g., as in the singles and doubles (SD) CI), the Brillouin theorem is no longer satisfied. It is desirable to extend the simplicity and beauty of the HF/SECI theory up to the levels including electron correlations. We will show that these merits are kept, in the SAC/SAC-CI theory, at any stage up to the exact limit.

3. SAC theory for the ground state

SAC is an abbreviation for the symmetry adapted cluster, the meaning of which will become clear later. It belongs to the cluster expansion approach, which was originated in the statistical theory of interacting atoms,[17] then introduced by Sinanoglu[18] in the theory of electron correlations in atoms and molecules, and further developed by Primas,[19] Cizek,[20] and Paldus.[21]

Electron correlation is defined on the basis of the HF theory as

$$E^{\mathrm{corr}} = E^{\mathrm{exact}} - E^{\mathrm{HF}}, \tag{15a}$$

$$\chi^{\mathrm{corr}} = \Psi^{\mathrm{exact}} - \Psi^{\mathrm{HF}}, \tag{15b}$$

where 'exact' stands for the exact solution of the non-relativistic Schrödinger equation. Since the HF model is an independent particle model, electron correlations represent mainly the collisions of electrons scattering into unoccupied orbitals. We introduce an excitation operator $T_I^\dagger$ which represents such a collision. For example, a collision of two electrons belonging to the occupied orbital φ_i, resulting in the scattering into the unoccupied orbital φ_a, is represented by the excitation operator $T_{\bar{i}\bar{i}}^{\bar{a}\bar{a}}$,

$$T_{\bar{i}\bar{i}}^{\bar{a}\bar{a}} = a_{a\alpha}^\dagger a_{a\beta}^\dagger a_{i\alpha} a_{i\beta}, \tag{16a}$$

$$T_{\bar{i}\bar{i}}^{\bar{a}\bar{a}}|0\rangle = \| \varphi_1\alpha\varphi_1\beta...\varphi_a\alpha\varphi_a\beta...\varphi_n\alpha\varphi_n\beta \|, \tag{16b}$$

where $|0\rangle = \Psi_g^{\mathrm{HF}}$ given by Eq. (3).

Configuration interaction (CI) method is one of the most popular methods for including electron correlations. This method is based on the expansion theorem,[22] and the correlated wave function is expressed as

$$\Psi^{CI} = B_0|0\rangle + \sum_I B_I T_I^\dagger|0\rangle \ , \tag{17}$$

where B_I are expansion coefficients. This method is simple and exact, but is usually slowly converging, especially for excited states. The dimension of the configurations easily reaches to the order of 10^8, though many efficient algorithms for handling such large matrices are proposed.[23-25] Further, it is difficult to extract a physical meaning from such a large number of configurations. It is also difficult to solve many lower solutions of such a large matrix, which is necessary for studying shake-up spectra, for example.

The main factor of electron correlation is collisions of two electrons. In many electron systems, however, there is a chance for three, four and more electrons to collide each other. However, the probability for four electrons, for example, to actually collide at the same time and place is very small. Four electron collisions actually important are the products of pair collisions occurring at different places of the molecule. This is because the fluctuation potential for the electron correlation is very short range, in nature, as Sinanoglu has pointed out very clearly.[18] When we introduce a sum of the excitation operators as

$$T = \sum_I C_I T_I^\dagger \ , \tag{18}$$

the wave function including higher-order collisional effects is written as

$$\Psi_g = \left(1 + T + \frac{1}{2}T^2 + \frac{1}{6}T^3 + ...\right)|0\rangle \ , \tag{19}$$

where the terms T^2, T^3, etc., represent two pair collisions, three pair collisions, etc., and the factors 1/2, 1/6, etc., are due to the indistinguishability of pair collisions. Eq. (19) is more compactly written as

$$\Psi_g = \exp(T)|0\rangle \ , \tag{20}$$

which is the cluster expansion. The suffix g again stands for the ground state. The theory based on this expansion is called coupled cluster (CC) theory.[20] Hereafter, we call the term, $(1+T)|0\rangle$ as linked term and the term, $\left(\frac{1}{2}T^2 + \frac{1}{6}T^3 + ...\right)|0\rangle$ as unlinked term.

In the above formulation, we have introduced the operators $T_I^\dagger$ representing two electron excitations (pair collisions). However, generally speaking, this is just an example, and we may take any operators physically important. An important example is to choose T as a sum of all single excitation operators,

$$T^{(1)} = \sum_i^{occ} \sum_a^{unocc} C_i^a a_a^\dagger a_i \,. \tag{21}$$

where i and a stand for the general spin orbital. Then, we get Thouless theorem,[26] i.e.,

$$\Psi^{SD} = \mathcal{N} \exp\left(T^{(1)}\right)\Phi^{SD} \,, \tag{22}$$

where Φ^{SD} and Ψ^{SD} are different single determinants, $\mathcal{N}$ a normalization constant. This theorem states that the transformation of a single determinant to another one is expressed by the operator $\mathcal{N} \exp\left(T^{(1)}\right)$: the cluster expansion includes the *self-consistency of orbitals*.

We note that for open-shell systems, the single determinant Ψ^{SD} on the left hand side of Eq. (22) is not a restricted determinant, but an *unrestricted* one which is not an eigen function of the spin-squared operator S^2. Generally, the wave function of the CC theory is *not* an eigenfunction of S^2, as actually reported for the CCSD wave functions for doublet radicals.[27] In the linear expansions like CI, the solution of the secular equation is always symmetry-adapted, irrespective of the choice of the excited configurations, because the Hamiltonian is totally symmetric. However, this is not the case for the non-linear expansions like cluster expansion. Further, as explained below, coupled cluster expansion may involve a larger number of variables than that necessary for describing the state.[2]

These difficulties do not occur when we choose excitation operators to be symmetry adapted. We define an excitation operator $S_I^\dagger$ to be symmetry adapted when the configuration $S_I^\dagger|0\rangle$ is symmetry adapted. For totally symmetric singlet states, we define the symmetry adapted cluster (SAC) expansion as[1,2]

$$\Psi_g^{SAC} = \exp(S)|0\rangle \,, \tag{23}$$

where

$$S = \sum_I C_I S_I^\dagger \,. \tag{24}$$

Since $S_I^\dagger$ is totally symmetric, the unlinked terms of Eq. (23) are also totally symmetric. For open-shell states like doublet and triplet states, we need a symmetry projector Q as

$$\Psi_g^{SAC} = Q\exp(S)|0\rangle = \left[1 + S + Q\left(\frac{1}{2}S^2 + \frac{1}{6}S^3 + ...\right)\right]|0\rangle, \quad (25)$$

where $|0\rangle$ is a restricted determinant and Q applies only to the unlinked terms, since the linked term is already symmetry adapted. We have also formulated the SAC theory for excited states in a way slightly different from Eq. (25).[28]

The SAC expansion defined by Eq. (23) is thus different from the CC expansion given by Eq. (20). In Table 1, we summarized the differences in a schematic way.[2] Generally speaking, the number of the unknown variables necessary for describing a state is the number of the symmetry adapted configurations belonging to this symmetry. The SAC expansion involves just that number of variables, since the unknown variables C_I are associated with the symmetry-adapted operators, $S_I^\dagger$ (Eq. (24)). In the expansion (20), on the other hand, the operator T is symmetry non-adapted so that it generally involves a larger number of variables than necessary. For example, the particle-hole operators include singlet, triplet, etc., operators, though the state under consideration is singlet. Since the products of two triplet operators may include singlet ones, the unlinked terms may involve the unknown variables originating from the triplet space, and they are not projected out by the symmetry projector Q as applied in Eq. (25). Thus, the conventional cluster expansion may involve larger number of variables than that necessary for describing the state. This may cause a difficulty in solution. In Table 1, we have sketched the differences between the CC expansion given by Eq. (20) and the SAC expansion given by Eq. (23) or (25). For closed-shell states, the CC wave function may become identical with the SAC wave function if the instability does not occur in the CC wave function.

Table 1: Schematic summary of the differences of the SAC expansion from the conventional cluster expansions[a]

Expansion	Linked term	Unlinked term[b]	Number of independent variables[c]	Symmetry[d]	With $T^{(1)}$ or $S^{(1)}$ alone[e]
$\exp(T)\|0\rangle$	$T\|0\rangle$	$T_IT_J\|0\rangle$	Larger	Mixed	UHF
$Q\exp(T)\|0\rangle$	$QT\|0\rangle \rightarrow S\|0\rangle$	$QT_IT_J\|0\rangle$	Larger!	Pure	SEHF
$Q\exp(S)\|0\rangle$	$S\|0\rangle$	$QS_IS_J\|0\rangle$	Just as required	Pure	Pseudo-orbital

[a] The operators T_I are not symmetry-adapted, but the operators S_I are symmetry-adapted.
[b] Only the second-order unlinked terms are given.
[c] The number of the independent variables included in each expansion is compared with that necessary for the description of the system under consideration.
[d] Symmetry of the total wave function.
[e] This column gives the orbital theory which is equivalent with the cluster expansion including $T^{(1)}$ or $S^{(1)}$ alone. We assume that these cluster expansions are solved with the variational principle. SEHF stands for spin extended Hartree-Fock.

The Thouless' theorem suggests an existence of a new orbital theory based on the SAC expansion. We construct the wave function,

$$\Psi^{PO} = Q\exp\left(S^{(1)}\right)|0\rangle, \tag{26}$$

using only single excitation SAC operator $S^{(1)}$. This is called pseudo-orbital theory.[1,2,32] Though the unrestricted HF (UHF) theory and the spin-extended HF (SEHF) theory are shown to be inadequate for the description of spin density distributions,[29-31] the pseudo-orbital theory gives the spin densities which are free from such deficiencies.[32-35] However, later, it has been shown that electron correlations are very important for calculating reliable spin densities.[36-40] We note here that the SAC wave function was first given in the form of Eq. (26) in 1977[1] prior to the more general form of Eqs. (23) and (25) in 1978.[2]

We now consider the solution of the SAC theory. In the SAC expansion, the unknown variables C_I are associated to the linked excitation operators $S_I^\dagger$, so that we require the Schrödinger equation, $H - E_g\left|\Psi_g^{SAC}\right\rangle = 0$, within the space of the linked configurations as[4]

$$\langle 0|H - E_g\left|\Psi_g^{SAC}\right\rangle = 0\ , \tag{27a}$$

$$\langle 0|S_I(H - E_g)\left|\Psi_g^{SAC}\right\rangle = 0\ . \tag{27b}$$

We have the same number of equations as the number of the unknown variables. This solution is called non-variational solution.

The variational solution is obtained by applying the variational principle to the SAC wave function and we obtain,[2,4]

$$\left\langle\Psi_g^{SAC}\right|H - E_g\left|\Psi_g^{SAC}\right\rangle = 0\ , \tag{28a}$$

$$\left\langle\Psi_g^{SAC}\right|(H - E_g)S_I^\dagger\left|\Psi_g^{SAC}\right\rangle = 0\ . \tag{28b}$$

This equation is valid *only* for the SAC expansion, but not for the CC expansion, because of the reasons summarized in Table 1. Generally speaking, the variational solution is more difficult than the non-variational one, because the former involves the integrals between the unlinked terms. However, we believe, as long as the wave function itself is accurate, the difference between the variational and non-variational solutions should be small.

We note that Eq. (28b) is the *generalized Brillouin theorem*. In comparison with Eq. (6a), Ψ_g^{SAC} corresponds to Ψ_g^{HF} and $S_I^\dagger\left|\Psi_g^{SAC}\right\rangle$ does to Φ_i^a. As the Brillouin theorem is a key equation in the HF/SECI theory, the generalized Brillouin theorem given by Eq. (28b) is a key equation in the theoretical framework of the SAC/SAC-CI theory. We will show this in the next section.

The SAC theory has the following properties. The first three are common to the CC theory.

(1) It effectively involves higher-order effects of electron collisions. It describes dynamic correlations quite effectively.[18]

(2) It is size consistent[41] or size extensive,[42] so that it correctly describes the energy change in the dissociation process such as $X_n \rightarrow nX$. This property is a direct consequence of the exponential ansatz, since

$$\exp(A)\exp(B) = \exp(A+B) \ , \tag{29}$$

when the operators A and B are commutable. This equation also implies that the correlations included in the cluster expansion is *separable* in the sense of Primas.[19]

(3) It includes self-consistency. This property is best represented by the Thouless' theorem given by Eq. (22). It guarantees that the cluster expansion is *independent* of a choice of the reference orbitals, when we include all the single excitation operators.

(4) The SAC theory defines not only the SAC wave function itself Ψ_g^{SAC} for the ground state, but also the excited functions which span the basis for excited states.[3] The SAC-CI theory is based on this property, and we explain it in the next section. This property is probably the most important property, among others, and is valid only for the SAC theory.

4. SAC-CI theory for excited, ionized, and electron attached states

It was thought for a long time that the description of electron correlations in excited states is much more difficult than that in the ground state. Excited states are generally open shells and are not represented by a single Slater determinant. Many different states of many different symmetries and natures are involved in a narrow energy range, which makes it difficult to suppose a single general theory in a useful form. However, this is not the case in the SAC-CI theory. By using the SAC-CI method, we can *easily* calculate the correlated wave functions of the excited, ionized and electron attached states,[3,4] as explained in this section.

We describe the electron correlations in the excited state on the basis of those in the ground state. Approximately speaking, excitations and ionizations involve only one or two electrons, and most other electrons lie essentially in the same orbitals as in the ground state. Therefore, the electron correlations in the excited state should be able to be compactly described by considering only some modifications to the ground-state electron correlations.

Let us define the excited functions $\{\Phi_K\}$ by using the SAC wave function as

$$\Phi_K = PS_K^\dagger \Psi_g^{SAC}, \tag{30}$$

where P is the operator which projects out the ground state wave function,

$$P = 1 - |\Psi_g^{SAC}\rangle\langle\Psi_g^{SAC}|, \tag{31}$$

and $\{S_K^\dagger\}$ a set of the excitation operators involving the excitations under consideration in a orbital picture. From the generalized Brillouin theorem of the SAC theory, Eq. (28b), it is easily shown that the functions $\{\Phi_K\}$ satisfy

$$\langle \Phi_K | \Psi_g^{SAC} \rangle = 0, \qquad \langle \Phi_K | H | \Psi_g^{SAC} \rangle = 0. \tag{32}$$

These equations imply, as Eq. (2) shows, that *the set of the functions* $\{\Phi_K\}$ *spans the space for the excited states*. We therefore describe the excited state *by a linear combination* of the functions $\{\Phi_K\}$,

$$\Psi_e^{SAC-CI} = \sum_K d_K \Phi_K , \tag{33}$$

which is the SAC-CI theory.[3]

Obviously, the SAC-CI wave function for the excited state satisfies the correct relations with the SAC ground state,

$$\langle \Psi_g^{SAC} | \Psi_e^{SAC-CI} \rangle = 0, \qquad \langle \Psi_g^{SAC} | H | \Psi_e^{SAC-CI} \rangle = 0 . \tag{34}$$

Applying the variational principle to Eq. (33) for solving the unknown variables $\{d_K\}$, we obtain

$$\langle \Phi_K | H - E_e | \Psi_e^{SAC-CI} \rangle = 0 . \tag{35}$$

Different solutions of Eq. (34), which correspond to different excited states, satisfy

$$\langle \Psi_e^{SAC-CI} | \Psi_f^{SAC-CI} \rangle = 0, \qquad \langle \Psi_e^{SAC-CI} | H | \Psi_f^{SAC-CI} \rangle = 0 , \tag{36}$$

since they are the solutions of the common secular equation. Thus, the SAC-CI wave function satisfies the correct relations with the ground state and with the other excited states. This is very important when we consider the properties, like transitions and relaxations, which interconnect different states.

In the above formulation, we have considered implicitly the excited states having the same symmetry as the ground state. However, the SAC-CI theory is also valid for the excited states having different symmetries (e.g., triplet), and for the ionized and electron attached states. We generalize Eq. (30) as

$$\Phi_K = P R_K^\dagger \Psi_g^{SAC} \tag{37}$$

where $\{R_K^\dagger\}$ represents a set of excitation, ionization, and/or electron attachment operators. In any cases, Eqs. (32)-(36) are valid.

Though the above formulation of the SAC-CI theory is variational, non-variational formulation is also possible and has been given in Ref. [43] The non-variational SAC-CI solution is obtained by projecting the Schrödinger equation onto the space of the linked configurations,

$$\langle 0 | R_K (H - E_e) | \Psi_e^{SAC-CI} \rangle = 0 . \tag{38}$$

Referring to Eq. (27), we note that in the non-variational case, the SAC and the SAC-CI wave functions satisfy the common set of equations. In particular, when we consider the excited states belonging to the same symmetry as the ground state, the operators $\{R_K^\dagger\}$ in Eq. (37) are actually $\{S_I^\dagger\}$. The solutions of the Schrödinger equation belonging to different eigenvalues are orthogonal and Hamiltonian orthogonal. Therefore, we obtain Eqs. (34) and (36) within the space of the linked operators under consideration. These equations are quite important for the theoretical consistency of the different states under consideration.

Practically speaking, the non-variational solution is easier than the variational one by the reason similar to that stated for the SAC solution, but we have to diagonalize non-symmetric matrices. When we first coded the SAC-CI program, it was in 1978, there was no efficient method for diagonalizing non-symmetric matrices of large dimensions. Therefore, we had to prepare the algorithm of iterative diagonalizations of non-symmetric matrices,[44] extending the Davidson's algorithm for symmetric matrices.[45]

When we diagonalize non-symmetric matrices, we obtain both right-hand and left-hand eigenvectors. Note however that in the non-variational SAC-CI equation, Eq. (38), the SAC-CI wave function corresponds to the right-hand solution. The left-hand solution never appears as a physical wave function in the above formalism. Therefore, we use the right-hand solution as the SAC-CI wave function in calculating properties.

As the SAC theory is exact, the SAC-CI theory is also exact. Though the introduction of the SAC-CI theory so far given is rather formal and straightforward, it has some interesting physics. First, omitting the projector, or including the identity operator into $\{R_K\}$, we can write the SAC-CI wave function as

$$\Psi_e^{\mathrm{SAC-CI}} = \mathfrak{R}\Psi_g^{\mathrm{SAC}}, \tag{39a}$$

where the excitator $\mathfrak{R}$ (a kind of reaction operator) is defined as

$$\mathfrak{R} = \sum_K d_K R_K^\dagger . \tag{39b}$$

We already know that the SAC wave function well describes the electron correlation of the ground state. The excitator $\mathfrak{R}$ describes the excitation starting from the electron correlation involved in the SAC ground state Ψ_g^{SAC}.

Generally speaking, excitation is only one or two electron processes and most other electrons lie in the situations (orbitals) similar to those in the ground state. Therefore, it is clever to start from the ground-state electron correlation and describe only the modifications caused by the excitation. Eqs. (39a) and (39b) just represent such an idea, which is the *transferability* of electron correlations between ground and excited states. This method is much easier than calculating all of the electron correlations of each state from the beginning. Since the ground-state electron correlation is easier to calculate than the excited-state one, when we calculate from the beginning, we first calculate it by the

SAC method and then utilize it in the SAC-CI method for calculating the excited-state correlations based on its transferability. For this reason, the SAC-CI expansion is much easier and more rapidly convergent than ordinary CI.

The SAC-CI wave function is also written in the form

$$\Psi_e^{\mathrm{SAC-CI}} = \exp\left(\sum_I C_I S_I^\dagger\right)\sum_K d_K R_K^\dagger|0\rangle \tag{40}$$

which has the structure of multi-reference CI. The configurations $R_K^\dagger|0\rangle$ represent the reference configurations and the operator $\exp(\sum_I C_I S_I^\dagger)$ represents the excitations from these reference configurations. In the latter, we use the coefficients $\{C_I\}$ determined for the ground state, which is based on the transferability of electron correlations between the ground and excited states. The dimension of the SAC-CI method is the number of the reference configurations which are typically in the order of 10^3 - 10^5, not like limited to ~ 10. Therefore, in the SAC-CI method, there is almost no ambiguity in the choice of the 'main reference' configurations in contrast to the ordinary multi-reference CI method.

The SAC-CI method can be applied to various kinds of excited states by using appropriate excitation operators. We have applied it to the excited states, ionized states, and electron attached states having spin multiplicities of singlet, doublet, triplet, and up to septet, as explained below. An important merit is that we can calculate these different electronic states *in a same accuracy*. We *can directly compare* the energies and the wave functions of different electronic states: a property quite important and useful in actual applications. *Thus, using the SAC/SAC-CI method, we can study chemistry and physics involving the ground and excited states of various spin multiplicities.*

5. Theoretical framework: SAC/SAC-CI theory compared with HF/SECI theory

The SAC/SAC-CI theory has a beautiful theoretical framework in common with the HF/SECI theory. This is summarized schematically in Table 2. For the ground state, the HF equation is just equivalent with the Brillouin theorem with respect to the *single* excitation operators $s_i^\dagger$, while the generalized Brillouin theorem of the SAC theory is valid for any excitation operators $S_I^\dagger$. In the HF/SECI method, the excited state is described by a linear combination of the singly excited configurations, $\psi_k = s_k^\dagger \Psi_g^{\mathrm{HF}}$ which are orthogonal and Hamiltonian orthogonal to the HF ground state. In the SAC-CI theory, the excited states are described by a linear combination of $\{\Phi_K\}$ defined by Eq. (30) or (37), which are orthogonal and Hamiltonian orthogonal to the SAC ground state. In the HF/SECI theory, the theoretical consistency is valid *only within the single excitations*, as we already explained in the introduction but in the SAC/SAC-CI theory it is valid, in principle, *at any stage up to the exact limit*. Needless to say that this similarity shown in Table 2 is valid not only for excitations but also for ionizations and electron attachments.

In the framework of the HF theory, one often adopts a frozen-orbital approximation, in which an excited state is represented by a single function ψ_k. Similarly, we may approximate an excited

state by a single function Φ_K. This approximation may be called 'frozen-correlation' approximation, in which a *complete* transferability of electron correlations between ground and excited states is assumed.

Table 2: Analogy in the theoretical framework between the HF/SECI theory and the SAC/SAC-CI theory.

	HF/SECI	SAC/SAC-CI
G		
R	HF	SAC
O	HF eq. = Brillouin Theorem	Generalized Brillouin Theorem
U	$\langle \Psi_g^{HF} \vert Hs_i^\dagger \vert \Psi_g^{HF} \rangle = 0$	$\langle \Psi_g^{SAC} \vert (H - E_g) S_I^\dagger \vert \Psi_g^{SAC} \rangle = 0$
N	$s_i^\dagger$; single excitation operator	$S_I^\dagger$; general excitation operator
D		
E	SECI	SAC-CI
X	$\psi_k = s_k^\dagger \Psi_g^{HF}$	$\Phi_K = PS_K^\dagger \Psi_g^{SAC}$
C	$\langle \psi_k \vert \Psi_g^{HF} \rangle = 0$	$\langle \Phi_K \vert \Psi_g^{SAC} \rangle = 0$
I	$\langle \psi_k \vert H \vert \Psi_g^{HF} \rangle = 0$	$\langle \Phi_K \vert H \vert \Psi_g^{SAC} \rangle = 0$
T	$\Psi_e^{SECI} = \sum_k d_k \psi_k$	$\Psi_e^{SAC\text{-}CI} = \sum_K d_K \Phi_K$
E	theoretically consistent *only*	theoretically consistent *at any*
D	*within single excitations*	*stage up to exact limit*
	$\Psi_e \cong$ single ψ_k	$\Psi_e \cong$ single Φ_K
	"frozen-orbital approximation"	"frozen-correlation approximation"

6. SAC/SAC-CI code

After completing the SAC/SAC-CI theory in 1978, I immediately started to write up a computer code. We already wrote about four different versions and the third one is SAC85.[14,15] The earlier two versions[46,47] were theoretically more accurate. The current versions, the fourth one,[16] is more efficient than before particularly in integral evaluations and diagonalizations. We are currently making the code more user-friendly and it will be published soon.

A remarkable merit of the SAC-CI method lies in its wide applicability to different electronic states and in its rather constant accuracy. Figure 1 shows the electronic states covered by the current SAC/SAC-CI code.[14-16] Using the SAC method, we calculate a closed-shell state of a molecule, and using the SAC-CI method, we calculate many different electronic states of the molecule, shown in Figure 1, which are produced by the excitations, ionizations, and electron attachments from/to the closed-shell state. Using the current SAC-CI code, we can study the ground and excited states having singlet to septet spin multiplicities. The subjects of the SAC/SAC-CI method are the *chemistry and physics involved in many different states shown in Figure 1.*

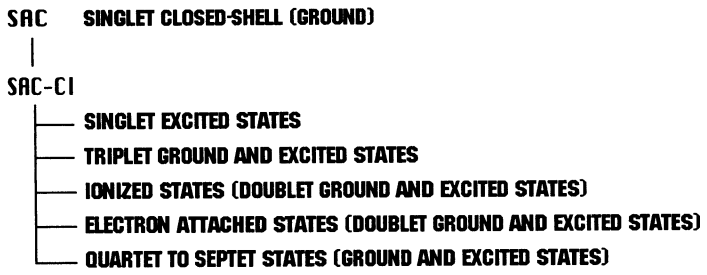

Figure 1: Electronic states studied by the current SAC/SAC-CI codes.

In most applications, the SAC solution is the ground state and the SAC-CI solutions are the excited states (in a general sense). However, when we calculate a doublet state, for example, we first calculate a closed-shell state by the SAC method by adding or by subtracting an electron from the molecule. The orbitals used in the SAC/SAC-CI calculations may be the open-shell RHF MOs of the doublet radical or the closed-shell RHF MOs for the anion or the cation. We already know that the orbital dependencies are small.

The SAC/SAC-CI theory itself is an exact theory. As you noticed in this review, the theory itself is quite simple and perspective. However, when we write up a code along the SAC/SAC-CI theory for actually calculating the ground and excited states, we have to introduce some approximations. We explain below the algorithms adopted in the present SAC-CI code currently used.

We explain first the SAC method.[2,4,5] We calculate a closed-shell state by this method as seen from Figure 1. Next, we explain the SAC-CI method.[3,4] We explain the SAC-CI SD (singles and doubles) method for calculating singlet excited states, triplet ground and excited states, ionized ground and excited states, and electron attached (ground and excited) states.[5,48] Next we explain the SAC-CI method for high-spin multiplicities,[7] namely, for the ground and excited states having quartet, quintet, sextet, and septet spin states. Then, we explain the SAC-CI general-R method[6] which is useful for studying more-than-two electron processes such as the shake-up processes in the ionization spectrum.

6.1. SAC method

We calculate singlet-closed shell state using the SAC theory. We include in the linked terms totally symmetric single and double excitation operators of the forms

single excitation, $$S_i^a = \left(a_{a\alpha}^\dagger a_{i\alpha} + a_{a\beta}^\dagger a_{i\beta}\right)/\sqrt{2} \qquad (41)$$

double excitation, $$S_{ij}^{ab} = S_i^a S_j^b \tag{42}$$

and in the unlinked terms the products of only the double excitation operators, which are quadruple excitation operators,

quadruple excitation, $$S_i^a S_j^b S_k^c S_l^d . \tag{43}$$

The triple excitations are known to be less important than the quadruple excitations which represent simultaneous occurrence of two pair collisions. We use the suffices, *i, j, k, l* for occupied orbitals and *a, b, c, d* for unoccupied orbitals in the reference single determinant (usually HF one). We adopt non-variational solution, for simplicity, so that we need integrals only up to linked × unlinked, and we need not to consider the unlinked terms higher than the third order.

We introduce the following approximations for reducing computational time. The number of linked operators is reduced by the configuration selection technique[48] which is popular in CI calculations.[23] This is effective for saving a storage and cpu time of computers. Namely,

(a) all single excitation operators are included,

(b) the double excitation operator $S_i^a S_j^b$ is included when its second-order contribution to the energy is larger than a given threshold λ_g; i.e.,

$$|\Delta E_s| \geq \lambda_g \tag{44}$$

where

$$\Delta E_s = \left|\langle 0|H|\Phi_{ij}^{ab}\rangle\right|^2 \Big/ \left(\langle \Phi_{ij}^{ab}|H|\Phi_{ij}^{ab}\rangle - \langle 0|H|0\rangle\right) \tag{45}$$

with

$$\Phi_s \equiv \Phi_{ij}^{ab} = S_i^a S_j^b |0\rangle . \tag{46}$$

For the unlinked terms, we include the products of the linked operators whose coefficients in the SDCI are larger than a given threshold, ζ_g, which is usually 10^{-3} - 10^{-2}.

The SAC solution is carried out by the non-variational procedure, though a code is given for an approximate variational procedure[5] which was less satisfactory than the non-variational one.

6.2. SAC-CI SD method

We explain here the SAC-CI SD method for the excited, ionized, and electron attached states having the spin multiplicities of singlet, doublet, and triplet. The SAC-CI wave function is written as

$$\Psi_e^{SAC-CI} = \sum_K d_K R_K^\dagger \exp\left(\sum_I C_I S_I^\dagger\right)|0\rangle \tag{47}$$

where the operators $\{S_I^\dagger\}$ and their coefficients $\{C_I\}$ are transferred from the SAC calculation for the ground state. The SAC-CI operators $R_K^\dagger$ are restricted here to single and double (SD) excitation operators which are shown in Table 3. Generally speaking, the excitation order of the operators $R_K^\dagger$ should be higher by one, at least, than the order of the real excitations to be calculated. For ordinary single excitation and ionization processes, this choice of the SAC-CI operators is sufficient. For multiple excitation processes, like shake-up ionizations, the inclusion of triple, quadruple, and higher excitation operators in the linked term is necessary and we call such method as general-*R* method,[6] which is explained in the next section.

Table 3: Single and double excitation operators for singlet and triplet excitations, ionization and electron attachment[a]

Type of excitation	Single excitation operator	Double excitation operator
Singlet excitation	$S_i^a = (a_{a\alpha}^\dagger a_{i\alpha} + a_{a\beta}^\dagger a_{i\beta})/\sqrt{2}$	$S_i^a S_j^b$
Triplet excitation	$T_i^a = a_{a\alpha}^\dagger a_{i\beta}$	$T_i^a S_j^b$
Ionization	$I_i = a_{i\beta}$	$I_i S_j^b$
Electron attachment	$A^a = a_{a\alpha}^\dagger$	$A^a S_j^b$

[a] i, j and a, b denote occupied and unoccupied orbitals, respectively, in the reference configuration $|0\rangle$.

For the unlinked terms, we include the terms

$$\text{single } R_K^\dagger \times \text{double } S_I^\dagger = \text{triple excitation} \tag{48}$$

for single electron processes such as ordinary excitations and ionizations, and further the terms

$$\text{double } R_K^\dagger \times \text{double } S_I^\dagger = \text{quadruple excitation} \tag{49}$$

for more accurate calculations and for two electron processes such as shake-up ionizations. The operators $S_I^\dagger$ are restricted to doubles since electron collisions are the main origin of the electron correlations. Note however that for two electron processes, the inclusion of some important triple excitation operators in the linked terms is more important and effective (economical) than including these unlinked quadruple excitation operators. For more details, see the SAC-CI general-*R* method given in the next section.

The configuration selection technique is also useful to reduce computer time.[48] For the linked $R_K^\dagger$ operators, (a) all single excitation operators are included and (b) double excitation operators are selected in the following way. Let $\Psi^{(p)}$ be a primary reference state

$$\Psi^{(p)} = \sum_i \alpha_i^{(p)} \Phi_i^{(p)}, \quad (p=1,\ldots,N), \tag{50}$$

which is usually a SECI solution or small SDCI solution. N is the number of the excited states we want to calculate. We denote doubly excited configuration to be selected as Φ_s and define

$$\Delta E_{si}^{(p)} = \left|H_{si}^{(p)}\right|^2 / \left(H_{ii}^{(p)} - H_{ss}\right) \tag{51}$$

where

$$H_{si}^{(p)} = \left\langle \Phi_s \middle| H \middle| \Phi_i^{(p)} \right\rangle,\ H_{ii}^{(p)} = \left\langle \Phi_i^{(p)} \middle| H \middle| \Phi_i^{(p)} \right\rangle,\ H_{ss} = \left\langle \Phi_s \middle| H \middle| \Phi_s \right\rangle . \tag{52}$$

We include only such Φ_s which satisfies

$$\left|\Delta E_{si}^{(p)}\right| \geq \lambda_e, \tag{53a}$$

with at least one of the configurations $\Phi_i^{(p)}$ whose coefficients $\alpha_i^{(p)}$ in Eq. (50) are larger than 0.1 or 0.05. Recently, we modified the condition, given by Eq. (53a) as[49]

$$\left|\alpha_i^{(p)}\right|^2 \left|\Delta E_{si}^{(p)}\right| \geq \lambda_e' . \tag{53b}$$

This equation takes into accounts the weight of the reference configurations in the primary states $\Psi^{(p)}$.

In the unlinked term $\sum d_K C_I R_K^\dagger S_I^\dagger |0\rangle$, we include only such double-excitation operators $S_I^\dagger$ whose coefficients in the ground-state CI are larger than 1×10^{-3} or 5×10^{-4}. As for the $R_K^\dagger$ operators in the unlinked term, two types of selections are possible. For single-electron processes, we included only single-excitation operators whose coefficients in the CI including only linked operators are larger than 0.1 or 0.05. The unlinked term then represents triple excitations. For two-electron processes like shake-up ionizations, we included single- *and* double-excitation operators whose coefficients in the CI including only linked operators are larger than 0.1, so that the unlinked term becomes triple *and* quadruple excitations. We referred to the former as '3-excited' calculations and the latter as '3,4-excited' calculations. However, for two electron processes, the inclusion of the triple and higher excitation operators by the general-R method is more effective than including '3,4-excited' terms, as shown below.

We note here a problem of the configuration selection method in calculating the potential curves of a reaction.[50] In such cases, an independent selection of operators for independent geometries may lead to a discontinuity of the calculated potential curves and properties. Therefore, we have adopted the following method of selections which we call GSUM (group sum) method. The GSUM method applies to both SAC and SAC-CI calculations.

An essential point of the GSUM method is to take a group sum of the operators (linked and unlinked) selected for all the representative points in the nuclear configuration space. We first select several representative points in the nuclear configuration space which cover the reaction under

consideration. The Hartree-Fock MO's of each geometry are rearranged so as to have the same ordering as the MO's of the adjacent geometries. The linked and unlinked operators are selected for each geometry, and then we take the group sum of these operators and the calculations are carried out at each geometry using the same set of this group sum of operators. This method is appropriate to study continuous changes in the potential energy curves and the properties along the change in nuclear configuration.

The SAC-CI solution is carried out by the non-variational method. We have also given an approximate variational procedure[6] in which the final matrices to be diagonalized are just the symmetrized ones of the non-variational ones. This method has been proved to give satisfactory results.

6.3. SAC-CI for high-spin multiplicity

High-spin multiplet states sometimes occur in molecules with degenerate or quasi-degenerate orbital structures. Transition metal clusters and complexes often have high-spin multiplicities in their ground and lower excited states. Other interesting examples are organic ferromagnetic molecules: high-spin organic ferromagnetic molecules having topological degeneracy due to methylene and phenylene components have been synthesized by Itoh, Iwamura, et al.[51,52] High-spin multiplet states are also important in the excited states. They often play an important role in the dynamic processes like predissociation and recombination processes.

In many cases, high-spin molecules have different spin states (including low-spin states) lying closely to each other. Therefore, accurate information on the relative stability is very important for assignments and for studying dynamics. However, these molecules are sometimes so large and the inclusion of both spin and electron correlations is important. Therefore, we need a theory that is useful and yet accurate for both low- and high-spin multiplicities.

The SAC/SAC-CI theory was originally formulated for arbitrary spin multiplicity, though in SAC85 the implementation has been limited up to triplet spin multiplicity. We explain here the SAC-CI calculations for the high-spin multiplicitites, quartet, quintet, sextet, and septet spin states. We start the correlated calculations from the SAC calculations for the closed-shell electronic configuration and generate high-spin states by applying the excitator $\mathfrak{R}$ to the resultant SAC wave function. Therefore, the lowest SAC-CI excitation operators are two-electron excitation operators for quartet and quintet multiplicities and three-electron excitation operators for sextet and septet spin states. In the sense of the SD-*R* method, these operators correspond to single excitation operators and therefore we have to include one-more (three- or four-) electron excitation operators in the linked operators. Table 4 shows the linked operators for the quartet to septet-spin multiplicities. The unlinked operators in the '3-excited' approximation are written as R(2)S(2) for quartet and quintet multiplicities and as R(3)S(2) for sextet and septet states, where S(2) represents the double excitation operators representing the electron correlation in the closed-shell ground state.

Table 4: Linked operators for the high-spin SAC-CI calculation.

Spin multiplicity	Linked operator[a,b]	
Quartet	$R(2) = R^{a}_{ij}$	$R(3) = S^{a}_{i} R^{b}_{jk}$
	$= a^{\dagger}_{a\alpha} a_{i\beta} a_{j\beta}$	
Quintet	$R(2) = R^{ab}_{ij}$	$R(3) = S^{a}_{i} R^{bc}_{jk}$
	$= a^{\dagger}_{a\alpha} a^{\dagger}_{b\alpha} a_{i\beta} a_{j\beta}$	
Sextet	$R(3) = R^{ab}_{ijk}$	$R(4) = S^{a}_{i} R^{bc}_{jkl}$
	$= a^{\dagger}_{a\alpha} a^{\dagger}_{b\alpha} a_{i\beta} a_{j\beta} a_{k\beta}$	
Septet	$R(3) = R^{abc}_{ijk}$	$R(4) = S^{a}_{i} R^{bcd}_{jkl}$
	$= a^{\dagger}_{a\alpha} a^{\dagger}_{b\alpha} a^{\dagger}_{c\alpha} a_{i\beta} a_{j\beta} a_{k\beta}$	

[a] The operator S^{a}_{i} denotes singlet-type single excitation operator defined in Table 3.

[b] Values in parentheses denote excitation levels relative to the closed-shell reference configuration.

6.4. Accuracy of the SAC-CI SD calculations

Tables 5 and 6 show the SAC/SAC-CI results for the singlet to septet excited states of N_2 and N_2^+ compared with the full-CI results. Table 5 corresponds to the results of Sections 6.1, 6.2 and Table 6 to those of Section 6.3 and they are taken from ref. [7]. The bond length is 1.09768Å for both N_2 and N_2^+, which is the equilibrium distance of the ground state of N_2. The basis set is [4s2p] Huzinaga-Dunning[53] plus Rydberg s function (ζ=0.028). The SAC/SAC-CI calculations are performed without configuration selection and the RHF MOs are used as reference MOs. For performing full-CI calculations, the active space is limited very small: five occupied and five unoccupied MOs.

Tables 5 and 6 show that the average discrepancies of the SAC-CI total energies from the full-CI ones are 4.21, 4.45, 3.42, 3.46, 2.27, 0.19, and 0.18 mhartrees, respectively, for the singlet, doublet, triplet, quartet, quintet, sextet, and septet states. They are small and the accuracies are rather constant independent of the multiplicity. For the excitation energy, the maximum deviation from the full-CI results is 0.15 eV.

The sizes of the SAC-CI calculations, which are the dimensions of the matrices involved, are small in comparison with those of the full-CI. In Table 5, the calculated excitation and ionization energies are compared with the experimental values. Despite that the sizes of the basis set and the active space are nothing but the test calculation quality, the calculated values compare reasonably well with the experimental values.

The excitation level shown in Tables 5 and 6 characterizes the nature of the excited state by the number of the electrons excited in the main configuration. For the singlet, doublet, and triplet excited states, they are unity, but two for the quartet and quintet states, and three for the sextet and septet states. These are the smallest possible numbers of excitations from the closed-shell SAC configuration.

Table 5: SAC-CI and full-CI results for singlet, doublet, and triplet states of N_2 and N_2^+.

State	Exitation level	Main configuration[a]	SAC-CI				Full-CI			Exptl.[d] (eV)
			Size	Total energy (Δ[b]) (au)		Excitation energy(Δ[c]) (eV)	Size	Total energy (au)	Excitaion energy (eV)	
Singlet states										
$X^1\Sigma_g^+$	0	0.97(22222)	72	-108.96314	(1.78)	0.0 -	2640	-108.96492	0.0	
$a^1\Pi_g$	1	0.95(222211)	34	-108.61413	(3.90)	9.50 (0.07)	2408	-108.61803	9.43	9.39
$a'^1\Sigma_u^-$	1	0.70(222121)+0.70(2212201)	26	-108.57018	(6.96)	10.69 (0.14)	2296	-108.57714	10.55	10.15-10.45
Average discrepancy					(4.21)	(0.11)				
Doublet states (Ionized)										
$X^2\Sigma_g^+$	1	0.95(22221)	21	-108.38866	(-0.49)	15.63 (-0.06)	3596	-108.38817	15.69	15.60
$A^2\Pi_u$	1	0.97(22122)	13	-108.31827	(5.47)	17.55 (0.10)	3460	-108.32374	17.45	16.98
$B^2\Sigma_u^+$	1	0.91(21222)	27	-108.26169	(7.38)	19.09 (0.15)	3596	-108.26907	18.94	18.78
Average discrepancy					(4.45)	(0.07)				
Triplet states										
$A^3\Sigma_u^+$	1	0.70(221221)+0.70(2221201)	63	-108.65943	(2.98)	8.26 (0.03)	3788	-108.66241	8.23	7.86
$B^3\Pi_g$	1	0.96(222211)	50	-108.66070	(2.96)	8.23 (0.03)	3720	-108.66366	8.20	8.12
$W^3\Delta_u$	1	0.70(222121)-0.70(2212201)	63	-108.61270	(5.65)	9.54 (0.11)	3788	-108.61835	9.43	9.15-9.3
$C^3\Pi_u$	1	0.93(2122201)	58	-108.53963	(5.09)	11.52 (0.09)	3720	-108.54472	11.43	11.25
$E^3\Sigma_g^+$	1	0.94(222210001)	62	-108.51327	(-0.44)	12.24 (0.06)	3688	-108.51283	12.30	11.95-12.0
Average discrepancy					(3.42)	(0.05)				

[a] The MO ordering is $(\sigma_g)(\sigma_u)(p_x\pi_u)(p_y\pi_u)(p\sigma_g)(p_x\pi_g)(p_y\pi_g)(p\sigma_u)$(Rydberg $s\sigma_g$)(Rydberg $s\sigma_u$)
[b] Deviation from the full-CI results (in mhartree).
[c] Deviation from the full-CI results (in eV).
[d] Reference 7

Table 6: SAC-CI and full-CI results for quartet, quintet, sextet, and septet states of N_2 and N_2^+.

State	Excitation level	Main configuration[a]	SAC-CI Size	SAC-CI Energy	Full-CI Size	Full-CI Energy	Difference (mhartree)
Quartet states (Ion)[b]							
$1^4\Sigma_u^+$	2	0.68(222110001)+0.68(22121001)	89	-108.07606	2416	-108.07561	-0.45
$1^4\Delta_u$	2	0.68(22211001)+0.68(221210001)	87	-108.02787	2524	-108.03024	2.37
$1^4\Pi_u$	2	0.96(212210001)	87	-108.00566	2480	-108.01184	6.18
$1^4\Sigma_u^-$	2	0.68(22211001)-0.68(221210001)	87	-108.00257	2524	-108.00787	5.30
$1^4\Pi_g$	2	0.98(221120001)	89	-107.97544	2480	-107.97792	2.48
$1^4\Sigma_g^+$	2	0.66(21122001)+0.66(212120001)	85	-107.96563	2524	-107.96668	1.05
$1^4\Delta_g$	2	0.66(21122001)-0.66(212120001)	87	-107.91663	2416	-107.91995	3.32
$1^4\Sigma_g^-$	2	0.66(21212001)-0.66(211220001)	85	-107.89388	2524	-107.90043	6.55
Average discrepancy							3.46
Quintet states[c]							
$1^5\Pi_u$	2	0.98(221210011)	128	-108.37714	1540	-108.37756	0.42
$1^5\Sigma_g^+$	2	1.00(221120011)	124	-108.35819	1540	-108.35838	0.19
$1^5\Sigma_u^-$	2	0.98(212210011)	128	-108.34024	1580	-108.34665	6.41
$1^5\Pi_g$	2	0.95(212120011)	120	-108.26921	1540	-108.26999	0.78
$1^5\Sigma_u^+$	2	0.68(22121101)+0.68(222111001)	116	-108.20347	1515	-108.20611	2.64
$2^5\Sigma_g^+$	2	0.65(222110101)+0.65(22121011)	124	-108.16790	1540	-108.17082	2.92
$1^5\Delta_u$	2	0.68(22211101)+0.68(221211001)	116	-108.16048	1515	-108.16045	-0.03
$2^5\Pi_u$	2	0.96(212211001)	128	-108.13264	1540	-108.13890	6.26
$1^5\Delta_g$	2	0.65(222110101)-0.65(22121011)	124	-108.12478	1540	-108.12485	0.07
$2^5\Pi_g$	2	0.90(221121001)-0.38(21221011)	120	-108.10537	1540	-108.10831	2.94
Average discrepancy							2.27
Sextet states (Ion)[d]							
$1^6\Pi_g$	3	0.99(212110011)	98	-107.76082	615	-107.76120	0.38
$1^6\Sigma_g^+$	3	0.97(221110011)	98	-107.74308	629	-107.74322	0.14
$1^6\Sigma_u^+$	3	0.99(211120011)	96	-107.62994	629	-107.62988	-0.06
Average discrepancy							0.19
Septet state[e]							
$1^7\Sigma_u^+$	3	0.91(221110111)	80	-107.84480	287	-107.84498	0.18

[a] The MO ordering is $(\sigma_g)(\sigma_u)(p_x\pi_u)(p_y\pi_u)(p\sigma_g)$(Rydberg $s\sigma_g$)(Rydberg $s\sigma_u$)$(p_x\pi_g)(p_y\pi_g)(p\sigma_u)$.
[b] Quartet states which dissociate to $N(^4S^0) + N^+(^3P)$ and $N(^4S^0) + N^+(^1D)$.
[c] Quintet states which dissociate to $N(^4S^0) + N(^4S^0)$, $N(^4S^0) + N(^2D^0)$, and $N(^4S^0) + N(^2P^0)$.
[d] Sextet states which dissociate to $N(^4S^0) + N^+(^3P)$.
[e] Septet state which dissociates to $N(^4S^0) + N(^4S^0)$.

In Table 6, we examined eight quartet states which lie in a narrow energy region (within 0.18 au): nevertheless the SAC-CI results give the same correct ordering as the full-CI ones. The sizes of the SAC-CI calculations are only 85-89, while those of the full-CI are 2400-2500. This shows the efficiency of the SAC-CI method. For the quintet states, we calculated ten states lying within 0.27 au. The SAC-CI results again give correct ordering, though the lowest four states are valence excited states, while the following six states are Rydberg in nature.

We thus conclude that the SAC/SAC-CI method gives accurate and efficient descriptions of not only the low spin multiplicities but also the high spin multiplicities. Similar examples were given in ref. [10, 54].

The exponentially generated (EG) CI method[55,56] explained briefly in Sec. 6.5.1 is also easily extended to high spin multiplicities. The method and the results were given in ref. [57].

6.5. SAC-CI general-*R* method

In many applications of the SAC-CI method, the excitator $\mathfrak{R}$ was expanded by single and double excitation operators. We know from the experiences that this choice gives accurate results when the excitations or ionizations under study involve only one-electron process. However, when we study two-or-more electron processes involved in excitations and ionizations, this choice is insufficient. We have to choose $R_K^\dagger$ operators to include not only the single and double (SD) excitation operators, but also triple-, quadruple-, and higher-excitation operators. We denote the former method as the SD-*R* method and the latter as the general-*R* method.[6]

In what cases, the general-*R* method becomes useful? The calculations of the ionization spectra are one such case. For lower ionizations, the Koopmans state is dominant so that the SD-*R* method is effective. But in a higher energy region, simultaneous ionization and excitation processes, typical two-electron processes, arise in the same energy region and mix with the one-electron Koopmans configurations. Therefore, in this region, it is necessary to calculate accurately both one- and two-electron processes. This is very important to obtain accurate results of not only energies but also intensities. Another interesting example of the two and many electron processes is the excited A_g states in polyene. In ethylene, its π-π^* state appears at about 8 eV. In butadiene, there is a chance of the occurrence of simultaneous excitations of the π electrons in the two double bonds. Such a chance increases further in long polyenes.

In both of the above cases, the ground state is well approximated by the Hartree-Fock configuration, so that the SAC method is well suited for the ground state: i.e., the ground-state is well described by a single reference SAC method. Therefore, these many-electron processes are well described by the SAC-CI method just by generalizing the $R_K^\dagger$ operators to include higher-excitation terms.

From the theoretical point of view, limiting the space of the $R_K^\dagger$ operators to be within singles and doubles is just one choice. Rather, in the spirit of the configuration selection, one may think it to be a better strategy to include *important* $R_K^\dagger$ operators *regardless* of their excitation numbers. In this point of view, the general-*R* method is a more natural choice than the SD method.

6.5.1. Generation of the higher-excitation operators

In the SD-*R* method, the double excitation operators are selected using the ordinary configuration selection algorithm explained in Section 8.2. However, if we adopt this algorithm for selecting triple, quadruple, etc. excited configurations, even the selection can be quite time-

consuming for moderate-size molecules. Instead, we recommend to use the algorithm developed in the EGCI (exponentially generated CI) method.[55,56]

The basic idea of the EGCI method is expressed by the script exponential operator as[55]

$$\Psi^{\mathrm{EGCI}} = \mathcal{EXP}\left(\sum_K a_K A_K^\dagger\right)\Phi_0, \tag{54}$$

$$\mathcal{EXP}\left(\sum_K a_K A_K^\dagger\right) = Q\left(a_0 + \sum_K a_K A_K^\dagger + \frac{1}{2}\sum_{K,L} a_{KL} A_K^\dagger A_L^\dagger + \ldots\right), \tag{55}$$

where the excitation operator $A_K^\dagger$ runs over all the space and spin symmetries and Q is a symmetry projector. Single and double excitation operators are usually adopted for the $A_K^\dagger$ operators. The constructions of the higher-order excitation operators are made in the spirit of the cluster expansion theory. Namely, the higher-order operators are generated as the products of the lower-order ones. For example, the important triple excitations would be the products of the single and double excitation operators which are important already in the SD-CI, and the important quadruple excitation operators would be the products of the already important double excitation operators in SDCI. In this way, the higher-order excitation operators are generated. We give independent coefficients, free from the lower-order ones, to these product operators. This is the spirit of the EGCI method.

In the above EGCI algorithm, the triple excitation operators are generated as follows. We first do SDCI for the states we are interested in and choose single excitation operators whose coefficients in the state vectors we are interested in are larger than a given threshold γ_S, and similarly choose double excitation operators whose coefficients are larger than a given threshold γ_D. By multiplying these single and double excitation operators, we obtain a space of triple excitation operators. We may use these triple excitation operators, or we may further diminish the space by applying the ordinary configuration selection method to these triple excitation operators. In the latter case, the preselection of the operators by the EGCI algorithm makes the ordinary selection procedure tractable in size. Similarly, we can generate quadruple and higher-excitation operators.

6.5.2. Result of the general-*R* method

We show the result of the general-*R* method applied to CO and C_2 from ref. [6]. We calculate a number of singlet and triplet excited states, ionized states and electron-attached states, and compare with the full CI results. The basis sets are the [4s2p] GTOs of Huzinaga and Dunning.[53] The active MOs are limited to four occupied and four unoccupied MOs for CO and four occupied and five unoccupied MOs for C_2.

Table 7 shows the full-CI and SAC-CI results for CO at its equilibrium bond length. 'Excitation level' denotes the number of electrons involved in the excitation, ionization, or electron-attachment process. 'Main configuration' shows the most important configuration in the full-CI,

Table 7: SAC-CI and full-CI results in hartree for CO at R = 1.1283Å (equilibrium distance)

State	Excitation level	Main configuration[a]	Full-CI		SAC-CI[b]					
					general-R			SD-R		
			size	energy	size	energy	$\Delta^c\times10^3$	size	energy	$\Delta^c\times10^3$
Singlet										
$^1\Sigma^+$	0	0.98(2222)	492	-112.74374	51	-112.74054	3.20	51	-112.74054	3.20
					106	-112.74353	0.21	51	-112.74045	3.29
$^1\Pi$	1	0.95(22211)	432	-112.41498	85	-112.41433	0.65	36	-112.41052	4.46
$^1\Sigma^-$	1	0.69(221210 - 212201)	408	-112.35612	56	-112.35662	-0.50	30	-112.35434	1.78
$^1\Delta$	1	0.68(212210 + 221201)	492	-112.35538	56	-112.35533	0.05	51	-112.35312	2.26
$^1\Pi$	1	0.89(12221)	432	-112.21458	85	-112.21264	1.94	36	-112.20864	5.94
$^1\Sigma^+$	1	0.92(2221001)	492	-112.20140	106	-112.19829	3.11	51	-112.19655	4.85
$^1\Sigma^+$	1	0.61(212210 - 221201)	492	-112.11498	106	-112.11449	0.49	51	-112.12178	-6.80
$^1\Pi$	2	0.64(221111)	432	-112.08857	85	-112.08731	1.26	36	-112.08426	4.31
		-0.49(21212 + 212102)					(1.27±1.14)[d]			(4.10±1.55)[d]
Triplet										
$^3\Pi$	1	0.96(22211)	392	-112.49703	95	-112.49644	0.59	44	-112.48977	7.26
$^3\Sigma^+$	1	0.69(21221 - 221201)	584	-112.40058	84	-112.40040	0.18	44	-112.40219	-1.61
$^3\Delta$	1	0.69(21221 + 221201)	584	-112.37771	84	-112.37756	0.15	44	-112.37747	0.24
$^3\Sigma^-$	1	0.68(22121 - 212201)	584	-112.36376	71	-112.36453	-0.77	40	-112.36188	1.88
$^3\Pi$	1	0.93(12221)	592	-112.26151	95	-112.25892	2.59	44	-112.25873	2.78
							(0.86±0.90)[d]			(2.75±2.40)[d]
Ion										
$^2\Sigma^+$	1	0.95(2221)	616	-112.22748	147	-112.22735	0.13	22	-112.22377	3.71
$^2\Pi$	1	0.96(2122)	588	-112.11220	143	-112.11346	-1.26	17	-112.11517	-2.97
$^2\Sigma^+$	1	0.93(1222)	616	-112.00829	147	-112.00904	-0.75	22	-112.00912	-0.83
$^2\Sigma^-$	2	0.68(22111) - 0.63(212101)	560	-111.82683	146	-111.82376	3.07	12	-111.78508	41.75
$^2\Delta$	2	0.57(21211 + 221101)	616	-111.82500	147	-111.82262	2.38	22	-111.77826	46.74
$^2\Pi$	2	0.78(22201) - 0.53(12211)	588	-111.81991	143	-111.81923	0.68	17	-111.76878	51.13
							(1.38±1.03)[d]			(24.52±22.20)[d]
Anion										
$^2\Pi$	1	0.97(22221)	588	-112.61520	84	-112.61375	1.45	17	-112.60802	7.18
$^2\Sigma^+$	1	0.97(2222001)	616	-112.44502	87	-112.44135	3.67	22	-112.43937	5.65
$^2\Delta$	2	0.68(222120 - 222102)	616	-112.35009	87	-112.34860	1.49	22	-112.32377	26.32
$^2\Sigma^+$	2	0.67(22212 + 222102)	616	-112.32870	87	-112.32651	2.19	22	-112.29876	29.94
$^2\Sigma^-$	2	0.81(222111)	560	-112.30504	64	-112.30248	2.56	12	-112.25951	45.53
							(2.27±0.82)[d]			(22.92±14.95)[d]

[a] The MO ordering is $(2s)(p\pi)(p\pi)(p\sigma)(p\pi^*)(p\pi^*)(2p\pi^*)(2p\sigma^*)$.
[b] The first row is the SAC result and all the others are the SAC-CI results.
[c] Δ shows the difference from the full CI result.
[d] (x±y) where x means the average discrepancy from the full-CI value and y means the standard deviation, both in millihartree.

and 'size' denotes the dimension of the matrices involved in the calculation. Δ shows the difference between the SAC-CI and full-CI energies in mhartree.

The SAC calculation is done for the singlet ground state and the result is commonly used in both general-R and SD-R SAC-CI methods. The second row shows the SAC-CI solution for the ground state.

Between the two SAC-CI methods, the general-R method gives the results which are superior to the SD-R method. This is clearly seen from the average discrepancy and the standard deviation

given in the parentheses. The accuracy of the general-*R* method is almost constant, independent of the excitations, ionizations, and electron attachments. The error is often negative, since the method of solution is nonvariational. The error of the SD-*R* method is larger than that of the general-*R* method, but for the single-electron processes, where the excitation level is unity, the results are acceptable. However, for the two-electron processes, the error is large, more than 20 mhartree, except for the $3^1\Pi$-singlet excited state. Thus, for two-electron processes, the SD-*R* method is poor and we have to use the general-*R* method.

The average discrepancy in the excitation energy, ionization energy, and electron affinity is calculated from the results shown in Table 7, and it is 0.025 eV for the general-*R* method. For the SD-*R* method, it is 0.067 eV for the single electron processes, but it is as large as 0.865 eV for the two-electron processes. We thus conclude that *the SAC-CI SD-R method is reliable only for single-electron processes. For two- and many-electron processes, we should use the general-R method.* We next examine the general-*R* method for C_2 molecule. Since the $p\sigma$-bonding MO is left unfilled in the low-lying region, the C_2 molecule has many doubly excited states in a relatively low-energy region. Table 8 shows the results of the SAC-CI general-*R* method as compared with the full-CI results. As seen from the excitation level, there are many two- and even three-electron processes. The errors of the general-*R* method are consistently small, independent of the excitation levels and the sizes of the matrices involved are much smaller than those of the full-CI.

Table 9 shows the excitation energies, ionization potentials and electron affinities of C_2 calculated from the results shown in Table 8. The average error from the full-CI results is 0.054 eV.

The C_2 molecule has unique excited, ionized and anion state due to the existence of the unfilled $p\sigma$ MO. The electronic structures and the spectroscopic properties of C_2 and C_2^- have received much experimental[58] and theoretical[59-62] attentions. In particular, the excitation energies are very small for several lower singlet and triplet states, and the electron affinity is *positive* for some lower anion states. The lowest excitation is for the $^3\Pi_u$ state. The calculated excitation energy is 0.528 eV in comparison with the adiabatic excitation energy of 0.09 eV.[58] The lowest doubly excited state is the $1^3\Sigma_g^-$ state, which is 1.92 eV above the ground state. The experimental adiabatic energy is only 0.80 eV above the ground state.[58] The existence of the stable excited states of the anion is particularly unique. Two anion states are calculated to be more stable than the neutral ground state. Experimentally, at least three adiabatic states of C_2^- seem to be lower than the neutral ground state.[58] In the ionized states, simultaneous excitation-ionization two- and even three-electron processes appear in a lower-energy region. However, because of the limitations in the active space and the basis set, detailed comparisons of the present results with experiment are limited.

We conclude from the present study that the accuracy of the SAC-CI method for two- and many-electron processes is improved by using the general-*R* method. For single-electron processes, the conventional SD-*R* method is reliable, as has already been confirmed.

Table 8: SAC-CI and full-CI results in hartree for C_2 at R = 1.24253 Å (equilibrium distance)

State	Excitation level	Main configuration[a] (C>0.3)	Full-CI size	Full-CI energy	SAC-CI (general-R)[b] size	SAC-CI (general-R)[b] energy	Δ[c]×10^3
Singlet							
$^1\Sigma_g^+$	0	0.85(2222)-0.35(20222)	748	-75.52629	46	-75.51985	6.44
					112	-75.52378	2.51
$^1\Pi_u$	1	0.96(22121)	654	-75.45297	86	-75.45147	1.50
$^1\Sigma_g^+$	2	0.63(22202 + 22022)-0.32(20222)	748	-75.42469	112	-75.42195	2.74
$^1\Delta_g$	2	0.68(22202 - 22022)	748	-75.42356	112	-75.42130	2.26
$^1\Pi_g$	2	0.90(21212)+0.36(2211101)	654	-75.32914	69	-75.32437	4.77
$^1\Sigma_u^+$	1	0.86(21221)	688	-75.30272	111	-75.30186	0.86
$^1\Sigma_g^+$	2	0.60(20222)+0.39(2222)-0.30(212111 - 2112101)	748	-75.25369	112	-75.24821	5.48
$^1\Sigma_u^-$	1	0.62(221201 - 2221001)	620	-75.22000	79	-75.21597	4.03
$^1\Delta_u$	1	0.63(221201)+0.62(2221001)	620	-75.20743	111	-75.20551	1.92
							(2.90±1.46)[d]
Triplet							
$^3\Pi_u$	1	0.94(22121)	950	-75.50716	158	-75.50437	2.79
$^3\Sigma_u^+$	1	0.91(21221)	960	-75.48006	152	-75.47606	4.00
$^3\Sigma_g^-$	2	0.96(22112)	940	-75.45908	95	-75.45324	5.84
$^3\Pi_g$	2	0.90(21212)	960	-75.42354	124	-75.41957	3.97
$^3\Sigma_u^+$	1	0.57(222101 - 2212001)+0.31(21221)	960	-75.28156	152	-75.27305	8.51
$^3\Delta_u$	1	0.62(2221001 + 2212001)	940	-75.25573	152	-75.24966	6.07
$^3\Pi_g$	2	0.80(2211101)+0.48(222011)	960	-75.23213	124	-75.22675	5.38
$^3\Sigma_u^-$	1	0.62(2221001+221201)	940	-75.23070	115	-75.22491	5.79
$^3\Pi_g$	2	0.59(2211101)+0.48(222011 - 220211)-0.34(2211101)	960	-75.19460	124	-75.18999	4.61
$^3\Sigma_g^+$	2	0.50(212111 - 2112101)-0.42(212111 - 2112101)	920	-75.19404	124	-75.18586	8.18
							(5.51±1.72)[d]
Cation							
$^2\Pi_u$	1	0.84(2212)-0.39(20122)	756	-75.06396	145	-75.05952	4.44
$^2\Delta_g$	2	0.66(22201 - 22021)	784	-74.99347	141	-74.99174	1.73
$^2\Sigma_g^+$	2	0.61(22201 + 22021)-0.37(20221)	784	-74.99019	141	-74.98752	2.67
$^2\Sigma_g^-$	2	0.82(22111)-0.48(22111)	728	-74.97066	109	-74.96650	4.16
$^2\Pi_g$	2	0.85(21211)	756	-74.96718	139	-74.96376	3.42
$^2\Sigma_u^+$	1	0.90(2122)	784	-74.96041	149	-74.95513	5.28
$^2\Pi_u$	3	0.89(22102)	756	-74.95202	145	-74.94621	5.81
$^2\Delta_u$	3	0.64(21202 - 21022)	728	-74.89972	123	-74.89819	1.53
$^2\Sigma_u^+$	3	0.61(21202 + 21022)	784	-74.86227	149	-74.86018	2.09
$^2\Sigma_g^+$	2	0.81(20221)	784	-74.84186	141	-74.83864	3.22
$^2\Sigma_u^-$	3	0.78(21112)+0.45(21112)	728	-74.83681	123	-74.83394	2.87
							(3.38±1.34)[d]
Anion							
$^2\Sigma_g^+$	1	0.93(22221)	1164	-75.57950	133	-75.57263	6.87
$^2\Pi_u$	2	0.96(22122)	1100	-75.54346	142	-75.54102	2.44
$^2\Sigma_u^+$	2	0.87(21222)	1144	-75.48444	121	-75.48003	4.41
$^2\Pi_g$	1	0.88(222201)	1100	-75.35620	125	-75.35020	6.00
$^2\Sigma_u^+$	2	0.64(222111 - 2212101)	1144	-75.32372	121	-75.31868	5.04
$^2\Sigma_u^-$	2	0.66(2221101)-0.50(221211)+0.45(221211)	1056	-75.32053	125	-75.31667	3.86
$^2\Pi_g$	3	0.78(2211201)+0.56(222021)	1100	-75.31882	125	-75.31391	4.91
$^2\Delta_u$	2	0.59(221211)+0.57(2221101)+0.35(2221101)+0.32(221211)	1056	-75.31794	121	-75.31379	4.15
$^2\Delta_u$	2	0.60(221211)-0.58(2221101)+0.36(2221101)-0.33(221211)	1056	-75.30293	125	-75.29987	3.06
$^2\Sigma_u^-$	2	0.65(2221101)-0.49(221211)+0.47(221211)	1056	-75.28780	125	-75.28073	7.07
							(4.78±1.45)[d]

[a] The MO ordering is (2s)(2sσ*)(pπ)(pπ)(pσ)(pπ*)(pπ*)(pσ*)(pσ').
[b] The first row is the SAC value and all the others are the SAC-CI values.
[c] Δ shows the difference from the full CI result.
[d] (x±y) where x means the average discrepancy from the full-CI value and y means the standard deviation, both in millihartree.

Table 9: Excitation energies, ionization potentials and electron affinities in eV calculated by the SAC-CI and full-CI methods for C_2 at R = 1.24253 Å (equilibrium distance)

State	Excitation level	Main configuration	Full-CI		SAC-CI (general-R)		
			size	energy	size	energy	$\Delta^c \times 10^3$
Singlet							
$^1\Sigma_g^-$	0	Hartree-Fock	748	0.0	112	0.0	0.0
$^1\Pi_u$	1	$p\pi \rightarrow p\sigma$	654	1.995	86	1.968	-0.027
$^1\Sigma_g^+$	2	$p\pi$, $p\pi \rightarrow p\sigma$, $p\sigma$	748	2.765	112	2.771	0.006
$^1\Delta_g$	2	$p\pi$, $p\pi \rightarrow p\sigma$, $p\sigma$	748	2.795	112	2.789	-0.007
$^1\Pi_g$	2	$2s\sigma^*$, $p\pi \rightarrow p\sigma$, $p\sigma$	654	5.365	69	5.426	0.061
$^1\Sigma_u^+$	1	$2s\sigma^* \rightarrow p\sigma$	688	6.084	111	6.039	-0.045
$^1\Sigma_g^+$	2	$2s\sigma^*$, $2s\sigma^* \rightarrow p\sigma$, $p\sigma$	748	7.418	112	7.499	0.081
$^1\Sigma_u^-$	1	$p\pi \rightarrow p\pi^*$	620	8.335	79	8.376	0.041
$^1\Delta_u$	1	$p\pi \rightarrow p\pi^*$	620	8.677	111	8.661	-0.016
							(0.036)[d]
Triplet							
$^3\Pi_u^-$	1	$p\pi \rightarrow p\sigma$	950	0.520	158	0.528	0.008
$^3\Sigma_u^+$	1	$2s\sigma^* \rightarrow p\sigma$	960	1.258	152	1.299	0.041
$^3\Sigma_g^-$	2	$p\pi$, $p\pi \rightarrow p\sigma$, $p\sigma$	940	1.829	95	1.920	0.091
$^3\Pi_g$	2	$2s\sigma^*$, $p\pi \rightarrow p\sigma$, $p\sigma$	960	2.796	124	2.836	0.040
$^3\Sigma_u^+$	1	$p\pi \rightarrow p\pi^*$	960	6.659	152	6.823	0.163
$^3\Delta_u$	1	$p\pi \rightarrow p\pi^*$	940	7.362	152	7.459	0.097
$^3\Pi_g$	2	$p\pi$, $p\pi \rightarrow p\sigma$, $p\pi^*$	960	8.005	124	8.083	0.078
$^3\Sigma_u^-$	1	$p\pi \rightarrow p\pi^*$	940	8.043	115	8.133	0.089
$^3\Pi_g$	2	$p\pi$, $p\pi \rightarrow p\sigma$, $p\pi^*$	960	9.026	124	9.083	0.057
$^3\Sigma_g^+$	2	$2s\sigma^*$, $p\pi \rightarrow p\sigma$, $p\pi^*$	920	9.041	124	9.195	0.154
							(0.082)[d]
Cation							
$^2\Pi_u$	1	$p\pi \rightarrow \infty$	756	12.581	145	12.633	0.053
$^2\Delta_g$	2	$p\pi$, $p\pi \rightarrow p\sigma$, ∞	784	14.499	141	14.478	-0.021
$^2\Sigma_g^+$	2	$p\pi$, $p\pi \rightarrow p\sigma$, ∞	784	14.588	141	14.592	0.004
$^2\Sigma_g^-$	2	$p\pi$, $p\pi \rightarrow p\sigma$, ∞	728	15.120	109	15.164	0.045
$^2\Pi_g$	2	$2s\sigma^*$, $p\pi \rightarrow p\sigma$, ∞	756	15.214	139	15.239	0.025
$^2\Sigma_u^+$	1	$2s\sigma^* \rightarrow \infty$	784	15.399	149	15.474	0.075
$^2\Pi_u$	3	$p\pi$, $p\pi$, $p\pi \rightarrow p\sigma$, $p\sigma$, ∞	756	15.627	145	15.717	0.090
$^2\Delta_u$	3	$2s\sigma^*$, $p\pi$, $p\pi \rightarrow p\sigma$, $p\sigma$, ∞	728	17.050	123	17.023	-0.027
$^2\Sigma_u^+$	3	$2s\sigma^*$, $p\pi$, $p\pi \rightarrow p\sigma$, $p\sigma$, ∞	784	18.069	149	18.058	-0.011
$^2\Sigma_g^+$	2	$2s\sigma^*$, $2s\sigma^* \rightarrow p\sigma$, ∞	784	18.624	141	18.644	0.019
$^2\Sigma_u^-$	3	$2s\sigma^*$, $p\pi$, $p\pi \rightarrow p\sigma$, $p\sigma$, ∞	728	18.762	123	18.772	0.010
							(0.035)[d]
Anion							
$^2\Sigma_g^+$	1	$\infty \rightarrow p\sigma$	1164	1.448	133	1.329	-0.119
$^2\Pi_u$	2	$p\pi$, $\infty \rightarrow p\sigma$, $p\sigma$	1100	0.467	142	0.469	0.002
$^2\Sigma_u^+$	2	$p\pi$, $\infty \rightarrow p\sigma$, $p\sigma$	1144	-1.138	121	-1.191	-0.052
$^2\Pi_g$	1	$\infty \rightarrow p\pi^*$	1100	-4.628	125	-4.723	-0.095
$^2\Sigma_u^+$	2	$p\pi$, $\infty \rightarrow p\sigma$, $p\pi^*$	1144	-5.512	121	-5.581	-0.069
$^2\Sigma_u^-$	2	$p\pi$, $\infty \rightarrow p\sigma$, $p\pi^*$	1056	-5.599	125	-5.636	-0.037
$^2\Pi_g$	3	$p\pi$, $p\pi$, $\infty \rightarrow p\sigma$, $p\sigma$, $p\pi^*$	1100	-5.646	125	-5.711	-0.065
$^2\Delta_u$	2	$p\pi$, $\infty \rightarrow p\sigma$, $p\pi^*$	1056	-5.670	121	-5.714	-0.045
$^2\Delta_u$	2	$p\pi$, $\infty \rightarrow p\sigma$, $p\pi^*$	1056	-6.078	125	-6.093	-0.015
$^2\Sigma_u^-$	2	$p\pi$, $\infty \rightarrow p\sigma$, $p\pi^*$	1056	-6.490	125	-6.614	-0.124
							(-0.062)[d]

[a] The Hartree-Fock MO ordering is $(2s)(2s\sigma^*)(p\pi)(p\pi)(p\sigma)(p\pi^*)(p\pi^*)(p\sigma^*)(p\sigma')$.
[b] Relative to the SAC-CI energy for the singlet ground state.
[c] Δ shows the difference from the full CI result.
[d] Average discrepancy

6.5.3. General-*R* method applied to ionization spectra

The results given in Tables 7-9 show a potential utility of the SAC-CI general-*R* method for the electronic processes including multi-electron processes. We show here an example of applications to the ionization spectra.

Figure 2 shows the ionization spectra of N_2 calculated by the SAC-CI SD and general-*R* method compared with the full-CI result.[63] Though the SD-*R* result gives rather good result for the lower three ionization peaks, which lie distantly from the satellite peaks, the results for the higher-energy peaks are not good. On the other hand, the general-*R* result is very close in all the energy region to the full-CI result. This is true not only in the energy but also in the intensity. The general-*R* result and the full-CI result almost exactly superpose each other, showing a high accuracy of the general-*R* method.

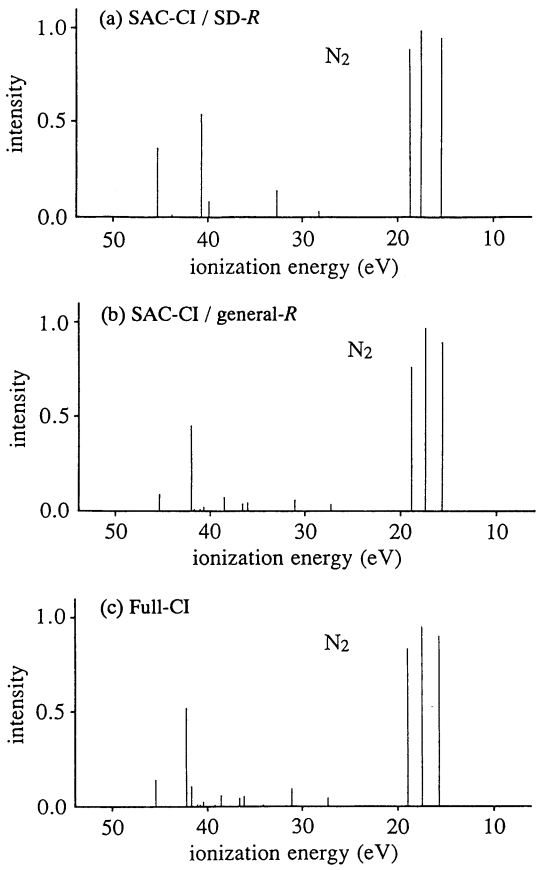

Figure 2: Ionization spectra of N_2 calculated by (a) SAC-CI SD-*R* method, (b) SAC-CI general-*R* method, and (c) full-CI method.

7. Multi-reference case : EGWF approach

The SAC theory assumes that the HF configuration is dominant in the expansion. The ground states of most molecules satisfy this condition. However, when a molecule undergoes homolytic dissociation, this situation may be broken down. For such cases, we have proposed MR(multi-reference)-SAC method[64,65] and applied it to the calculations of the potential energy curves of the ground and excited states of small molecules.[65] The underlying theoretical concept was further generalized as the exponentially generated wave function (EGWF) approach.[55] In this generalized idea, the MR-SAC wave function is just one of the multi-(or mixed-)exponentially generated (MEG) WFs.[55,66] When we get the MEG-WFs, we can construct on that basis the wave functions for excited, ionized, and electron-attached states, which we call EX(excited)-MEG WFs. In short, MEG and EX-MEG correspond to SAC and SAC-CI, respectively, in the single-reference limit and the thoeretical framework is similar. Coding of these methods was completed[67] and the test calculations gave satisfactory results.[65,66] We have also proposed a CI wave function constructed in the spirit of the EGWF and called it EGCI.[56] Applications of EGCI to high-spin molecules were also reported.[57] This method is a useful and reliable method for studying reaction dynamics. Though these EGWF approaches are quite interesting, we can not give a detail for a lack of the space.

8. Chemistry studied by the SAC/SAC-CI method

The SAC/SAC-CI method is already 18 years old and it has offered a practically useful way of studying many different topics in chemistry and physics.

A remarkable merit of the SAC-CI method lies in its wide applicability to different electronic states and in its rather constant accuracy. As shown in Section 6, our current SAC/SAC-CI code can deal with many different electronic states as shown in Figure 1. It also shows a promising future of the SAC/SAC-CI method.

In some topics of interest, we have to study many different electronic states at the same time. The dynamics in the excited states[68-72] and the (photochemical) reactions on surface[73-76] are such subjects. The SAC-CI method is suitable for such studies since it describes many different states as shown in Figure 2 in essentially the same accuracy. Examples showing such constant accuracy have been given in Tables 6-8. In conclusion, using the SAC/SAC-CI method, we can study *chemistry and physics involved in many different states* shown in Figure 1.

In Table 10, we summarize the subjects and the molecules studied so far using the SAC-CI method. After completing the SAC/SAC-CI first code, some calculations were for confirming the accuracy of the SAC/SAC-CI method, which were quite encouraging,[5] and later we applied it to the spectroscopies of valence and Rydberg excitations and ionizations. The molecules studied include organic and inorganic molecules, metal complexes, and more recently metallocenes and biologically important porphyrins. Benzene, pyridine, and naphthalene were the largest molecules ever calculated by accurate theories when we published the SAC-CI studies on the excited and ionized

Table 10: Chemistry and physics studied by the SAC/SAC-CI method

Subject	Publication	Reference
Theory		
SAC	JCP,1978; CPL,1979	2, 4, 5, 28, 48, 64
SAC-CI	CPL,1978,1979	3, 4, 5, 6, 7, 48, 77
Spectroscopy		
Valence and Rydberg Excitations		
Be	CPL,1979,1981	5, 28
BH_3	CPL,1979	5
H_2O	CPL,1979,1981,1991; IJQC,1981	5, 77, 28, 54
CH_2	CPL,1981	28
H_2CO	JCP,1981	78
CO_2,N_2O	CP,1983	48
NO	IJQC,1983	81
C_2H_2O	JCP,1983	84
NH_4^+	JACS,1984	83
CO, C_2	CPL,1991	6
Ethylene	JCP,1984; BCSJ,1996	82, 118
Pyrrole,Furan,Cyclopentadiene	JCP,1985	85
Pyridazine	CP,1986	86
Benzene	JCP,1987; TCA,1987	89, 65
Naphthalene	CPL,1987	90
Butadiene	CPL,1988	91
Pyridine	JCP,1988	92
Cyclopropane, Bicyclobutane, Propellane	CP,1996	119
Ionizations, Shake-up, and Electron-Attachment		
H_2O	CPL,1979,1982; IJQC,1981	5, 79, 77
H_2CO	JCP,1981	78
CO_2,N_2O	CP,1983	48
COS,CS_2	CP,1983	80
NO	IJQC,1983	81
CO, C_2	CPL,1991	6
Ethylene	JCP,1984	82
Pyrrole,Furan,Cyclopentadiene	JCP,1985	85
Benzene	JCP,1987	89
Naphthalene	CPL,1987	90
Pyridine	JCP,1988	92
Butene(cis, trans, iso-)	JCP,1995	107
CHCl=CHCl	J. Mol. Struc.	111
Hyperfine Splitting Constant and Spin Density		
BeH, CH_3, C_2H_5, HCO, $H_2C{=}CH_2$	JPC,1983 (GTO)	36
H_2O^+, H_2CO^+, $O(CH_3)_2^+$, CH_3NH, C_2H_5, CH_3O	JCP,1988 (GTO)	38
H_2^+, H_2O^+, $O(CH_3)_2^+$, H_2CO^+, CH_3, C_2H_5, CH_3NH, CH_3O, $H_2C{=}CH$, HCO	JCP,1989 (STO; with cusp)	39

(Table 3 continue)

(Table 3 continued)

Anisotoropy	JCP,1990		96
CH_3F^+	JCP,1991		97
$CFCl_2$	JCP,1991		98
NH_2	JCP,1992	(STO; with cusp)	101
OH,CH_2,BH_2,CH_3,H_2O^+	JCP,1994	(GTO, full CI)	40
High-Spin Molecules			
N_2, OH, m-phenylenebis(methylene)	JCP,1993		104
Potential Curve and Dynamics, Photochemistry			
Li_2, Li_2^+	Can.J.C.,1985		50
CO	Indian Aca. Sci. 1986		43
Ar_2, Ar_2^+	JCP,1990		68
CsXe, CsNe,CsAr,CsKr	CPL,1990; JCP,1994		69, 70
O_2^-,O_2^{2-}	CPL,1992		102
MnO_4^-	TCA,1994; JPC,1995		71
$Ni(CO)_4$	JCP,1995		72
Excitation and Ionization Spectra of Metal Complexes			
$MoO_{4-n}S_n^{2-}$	JCP,1990		94
RuO_4, OsO_4	IJQC,1991		95
MnO_4^-	JCP,1991		99
$TiCl_4,TiBr_4,TiI_4$	JCP,1992,1994		100, 106
CrO_2Cl_2	JCP,1993		104
CrO_4^{2-}	JCP,1994		105
$RhCl_6^{3-}$, $RhCl_5(H_2O)^{2-}$	BCSJ,1995		108
SnH_4, $Sn(CH_3)_4$	JPC,1995		109
TcO_4^-	TCA,1995		110
MoF_6	JPC,1996; IJQC,1996		117
Catalysis and Surface Photochemistry			
Pd_n-H_2	JACS,1985,1987		87
Pt_n-H_2	JCP,1988		93
Ag-O_2	CPL,1990; JCP,1993		73, 74
ZnO-H_2	IJQC,1992		103
$(Alkali)_n$-Cl_2	J.Mol.Cat.,1992		75
Pt_n-CO	JCP,1996		76
Spectroscopy of Large Systems			
Porphin ($C_{20}H_{14}N_4$)	JCP,1996		49
Mg porphin ($MgC_{20}H_{12}N_4$)	CPL,1996		112
Oxyheme ($FeC_{23}H_{16}N_6O_2$)	CPL,1996		113
Tetrazaporphin ($C_{16}H_{10}N_8$)	CPL,1996		114
Carboxyheme ($FeC_{24}H_{16}N_6O$)	CPL,1996		115
Phthalocyanine ($C_{32}H_{18}N_8$)	JPC,1996		116

states. We could improve the excited states having V character in comparison with the previous calculations by including a large amount of σ-electron correlations together with the π-electron ones. In particular, the SAC-CI calculations on metal porphyrins constitute the largest calculations ever made by the accurate ab initio method including electron correlations. We give a brief review later on this subject taking porphin, tetrazaporphin and carboxyheme as examples.

Surface chemistry is often a very good subject of the SAC/SAC-CI method since in catalysis, the active state and species does not necessarily correspond to the ground state, but sometimes involves the excited states of the system.[73,74,93] For example, oxygen exists in various forms on a metal surface. When we deal with them theoretically, one corresponds to the ground state but the other corresponds to the excited state.[73,74] Surface photochemistry is a field now growing up very rapidly. Cluster model was used in H_2/Pd,Pt and CO/Pt chemisorptions and photodesorptions, but in O_2/Ag and Cl_2/Na,K,Ru chemisorptions, the cluster model fails because it does not describe the effect of bulk metal. We have proposed dipped adcluster model (DAM)[120,121] in order to take into account the effect of free electrons of the metal and the surface image force as two important effects of the bulk metal and succeeded to quantitatively describe the O_2 and Cl_2 chemisorptions on the metal surfaces. In both cases, electron transfers from the metal surface to the admolecules were important. In the Cl_2/Na,K,Ru system, the chemisorption accompanies the surface luminescence and the surface electron emission, which were studied successfully by the SAC-CI method. The harpooning of an electron was satisfactorily described by the DAM.[75]

In the dynamics of the excited states, many different states are often involved and the SAC-CI method is useful. In the study of the potential curves of CO,[43] we showed a utility of the SAC-CI method in the region near the equilibrium distance. When the CO distance is large, the HF dominant $^1\Sigma$ state becomes an excited state. Then, we calculated the SAC wave function for that excited state, and calculated the ground state using the SAC-CI method. For Ar_2, the SAC-CI potential curves were shown to be very accurate.[68] An overview will be given in this review for the collision induced absorption spectroscopy of CsXe system.[69,70] Recently, the photochemical decompositions of MnO_4^{2-} and $Ni(CO)_4$ were studied by the SAC-CI method.[71,72]

Hyperfine splitting constant (hfsc) is an important property of doublet, triplet and high-spin molecules. The isotropic hfsc is represented by the Fermi contact interaction which is proportional to the spin density at the nucleus. Since this is a very local property, ab initio calculations of the hfsc's are more difficult than those of the other electronic properties such as dipole moment, polarizability, etc. The SAC-CI method is shown to give fairly accurate results for the hfsc's. It has been clarified that the following factors are important for adequate descriptions of the hfsc's;[36,39,40] (a) spin-polarization effect, (b) electron correlation effect, and (c) the cusp condition at the positions of nuclei.

We give in this review some recent topics of interests of the SAC-CI applications: excitation spectra of metal complexes, collision-induced absorption spectra of CsXe, and excited states of porphyrins. Some interesting previous topics were overviewed in a previous review article.[10]

9. Related methods

It is interesting to formulate the SAC-CI theory in a different way.[84] Starting from Eq. (39), it is easy to derive an equation-of-motion (EOM) type formula

$$[H,\mathfrak{R}]\Psi_g^{SAC} = \Delta E \mathfrak{R}\Psi_g^{SAC}, \tag{56}$$

where ΔE is the excitation energy

$$\Delta E = E_e^{SAC-CI} - E_g^{SAC}. \tag{57}$$

Eq. (56) is notable in that only the ground-state wave function is involved but we have the excitation energy. Rowe,[122] Shibuya, Mckoy, Yeager and others[123-125] have developed the EOM method for directly calculating the difference properties like transition energies and moments. We note that the so-called killer condition is unnecessary in the above formalism.

From Eq. (56), we can further derive

$$\langle 0|R_K e^{-S}[H,\mathfrak{R}]e^{S}|0\rangle = \Delta E \langle 0|R_K \mathfrak{R}|0\rangle \tag{58}$$

which is equivalent with the CCLR (coupled cluster linear response) equation recently investigated extensively by Koch and Jørgensen.[126,127] This line of theory can be traced back to Mukherjee.[128] This formulation shows that the SAC-CI method and the CCLR method are essentially equivalent. However, different formulations are sometimes quite useful, because different insights, though common, may be obtained from such formulations.

Recently, a method with a slight modification of SAC-CI was published with the name of equation-of-motion coupled-cluster (EOM-CC).[129,130] It does not start from the EOM formula like Eq. (56), but its formalism[130] is just the same as the SAC-CI one. Namely, it used in Eq. (39) the coupled cluster (CC) wave function (CCSD) instead of the SAC wave function and expanded the excitation operator $\mathfrak{R}$ by single and double excitation operators. For closed shells, if the instability does not occur in the CC theory, the CC wave function becomes the same as the SAC wave function, so that the EOM-CC is the same as the SAC-CI. Actually, the SAC-CI theory itself is exact and the difference is only minor: different approximations were adopted in practical calculations. The SAC/SAC-CI method is now well established, due to our pioneering efforts, not only as a theory for ground, excited, ionized, and electron-attached states, but also as a useful computational method for studying chemistry and physics involving these different electronic states. It is therefore misleading to use the term EOM-CC, since it is not new but published much (11 years) later after the SAC-CI method is established as a quite useful method, and since it is merely a modification of the SAC-CI method.

It is further nonsense to use the terms IP-EOMCC[131] and EA-EOMCC[132]: SAC-CI has been formulated from the beginning to apply not only to the excited states, but also to the ionized and electron attached states, and we have published many such applications for many years since 1979.[4,5] Our SAC-CI code[16] can deal with the ground and excited states having spin multiplicities

from singlet up to septet as shown in Figure 1. The EOM-CCSDT method[133] is also a special case of our SAC-CI general-*R* method published earlier.[6]

10. Excitation spectra of metal complexes

Metal complexes show beautiful colors in all possible ranges, and therefore, we thought at first that there should be a lot of studies on the excitation spectra of metal complexes. However, we soon found this was wrong. The reason was simple, there was no good theory for excited states before SAC-CI. Probably, metal complexes were too large for the theory already existed before.

We show here the SAC-CI study of the excitation and ionization spectra of $TiCl_4$,[100] $TiBr_4$, TiI_4,[106] CrO_2Cl_2,[104] and $Sn(CH_3)_4$.[109] We explain only the final results and for the details we refer to the original papers.

10.1. $TiCl_4$, $TiBr_4$, TiI_4

Figure 3 shows the experimental and SAC-CI theoretical excitation spectra of $TiCl_4$, a tetrahedral molecule. The lowest calculated state is $1T_1$ arising from the $1t_1 \rightarrow 2e$ (homo-lumo) transition, but this is dipole forbidden. The first allowed transition is to $1T_2$ which again arises from $1t_1 \rightarrow 2e$ transition. It is calculated at 4.42 eV in comparison with the experimental values, 4.43 and 4.41 eV: the first band is assigned to the $1T_2$ state. Similarly, all the peaks observed in the experimental spectrum are assigned to the dipole-allowed T_2 states as seen in Figure 3. We note that the peaks in the experimental spectrum are sometimes composed of the two or three transitions. For example, the large band at about 7 eV is assigned to be composed of the transitions to the $6T_2$, $7T_2$, and $8T_2$ states, the transition to the $8T_2$ state being the most intense one.

The nature of the transition is different in different energy regions. In the region of 4 - 6 eV, the excitation is mainly from the ligand to the metal-ligand anti-bonding MO, in the region of 6 - 8 eV, the excitation is from the metal-ligand bonding to the metal-ligand anti-bonding MO, and in the region of 8 - 11 eV, the excitation is essentially within the ligands, i.e., from the ligand lone-pair MO to the ligand Rydberg orbitals. The knowledge of the nature of the excitation is useful for understanding the reaction and the dynamics in which the excited state is involved.

We have studied the excitation spectra of many highly symmetric compounds, T_d and O_h, where the excitations often involve the transitions between degenerate orbitals. For example, the transitions $t_1 \leftrightarrow 2e$ give T_1 and T_2 symmetries. An important observation was that T_1 is always lower than T_2 as seen here for $TiCl_4$. This fact can be explained using the frozen orbital approximation (FZOA) and the orders of magnitudes of the repulsion integrals involved in the splitting of the degenerate transitions.[117] We have systematically shown the validity of FZOA in understanding the ordering and the intensities of the transitions involving two degenerate orbitals, and an example is given for the O_h complexes like MoF_6.[117]

We studied further the excitation and ionization spectra of $TiBr_4$ and TiI_4.[106] For these molecules, an interesting point is the effect of the spin-orbit interaction on the excitation and ionization spectra. On the right-hand-side of Figure 3, we show the SAC-CI excitation spectra of

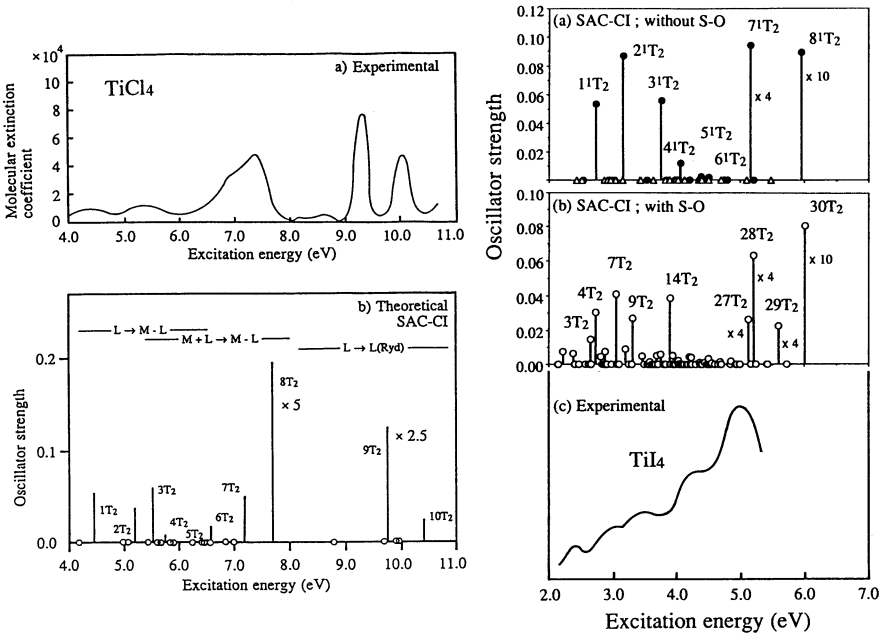

Figure 3: Left, Excitation spectra of $TiCl_4$ (a) experimental (b) SAC-CI theoretical. For the $8T_2$ and $9T_2$ states the intensities given for the SAC-CI spectrum are 1/5 and 2/5 of the calculated values. Right: Theoretical excitation spectra of TiI_4 (a) without spin-orbit interaction [singlet (•) and triplet (Δ) states]; (b) with spin-orbit interaction; and (c) experimental excitation spectrum.

TiI_4 without and with the spin-orbit interaction. We see that the spin-orbit interaction is very large and without it the peaks in the experimental spectrum are not well understood. For $TiBr_4$, the spin-orbit effect was not so large.

The spin-orbit interaction was considered in a very simple way. After finishing the SAC-CI calculations of the singlet and triplet excited states, we add spin-orbit integrals additionally and diagonalize again. For more details, see refs. [93] and [106].

10.2. CrO_2Cl_2

Figure 4 shows the experimental spectrum of chromyl chloride CrO_2Cl_2 compared with the theoretical spectrum calculated by the SAC-CI method.[104] The right-hand side is the spectrum in the lower-energy region and the left-hand side is for higher-energy region. Though we refer to the original paper for the detailed analysis, we see that the overall features of the experimental spectra is well reproduced by the SAC-CI theoretical spectra. For this molecule is C_{2v}, we have many dipole-allowed peaks in comparison with those of the highly symmetric molecules. Partially for this reason, the observed peaks are composed of many transitions. The nature of these transitions were given in ref. [104].

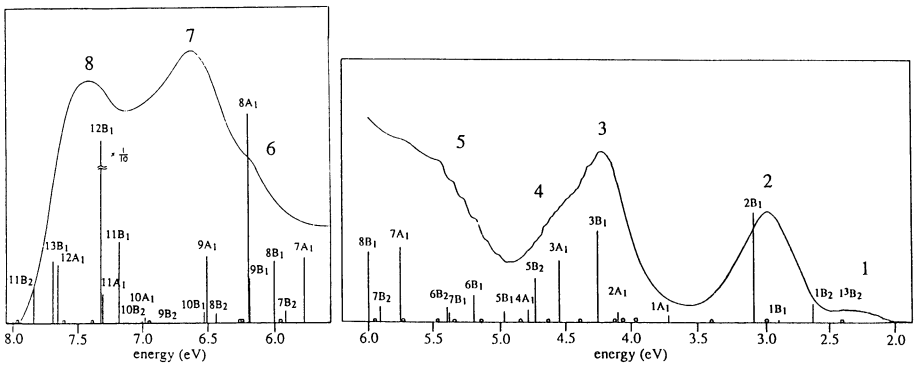

Figure 4: SAC-CI theoretical excitation spectrum of CrO_2Cl_2 compared with the experimental spectrum.[134]

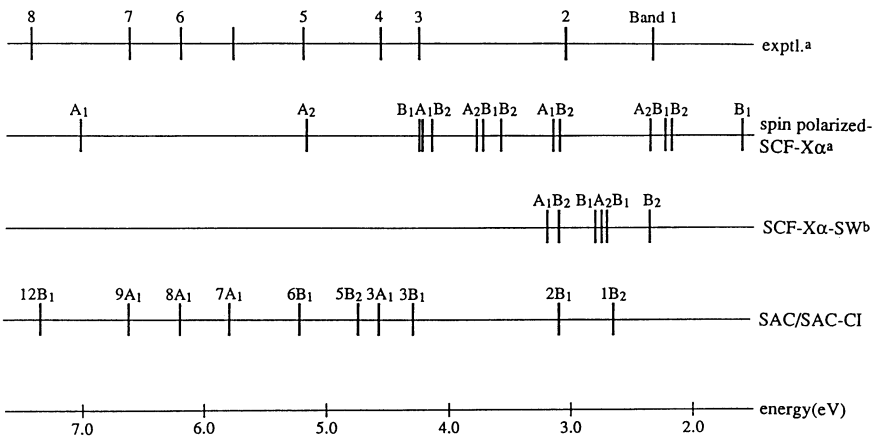

Figure 5: Summary of the ab initio calculations for the excitation energies of CrO_2Cl_2; (a) Jasinski et al.[134] (b) Miller, Tinti, and Case[135]

Figure 5 shows a comparison of the various ab initio theoretical results for the excitation spectrum of CrO_2Cl_2 with the experimental spectrum. Among the theoretical spectra, only the SAC-CI result agrees with the experimental peaks. The previous theoretical results are totally different from the experimental spectrum. This is one example showing why the spectra of transition-metal complexes were left unstudied before the SAC-CI method had appeared.

10.3. $Sn(CH_3)_4$

Lastly, we show an example of the Rydberg transitions. Figure 6 shows a comparison of the experimental and SAC-CI theoretical spectra of $Sn(CH_3)_4$ in 6 - 10 eV region.[109] The inset shows the spectrum calculated by Fernandez et al.[136] For calculating Rydberg transitions we have to include Rydberg basis sets: we included three Rydberg orbitals for each of the s, p, d orbitals of Sn and one Rydberg s, p orbitals for C. We see that the $1T_2$ and $8T_2$ excitations have very strong intensities, implying strong admixtures of valence excitations. Actually, the $1T_2$ state has a mixed nature of the 6s Rydberg orbital and Sn(s)-C(s) antibonding orbital. The $8T_2$ state also has a mixed nature of the 6d Rydberg orbital and the Sn(5p)-C(p) antibonding orbital. Other T_2 states are essentially the Rydberg states.

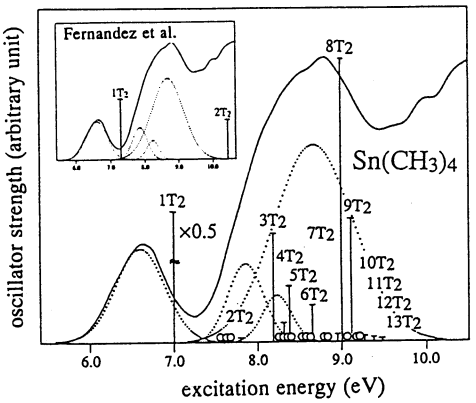

Figure 6: SAC-CI theoretical excitation spectrum of $Sn(CH_3)_4$ below the first IP, 9.70 eV, compared with the observed spectrum.[136] Inset is the spectrum calculated by Fernandez et al.[136]

We think that our SAC-CI spectrum compares well with the experimental spectrum. The first peak is the transition to the $1T_2$ state and the second broad peak includes a large number of Rydberg states, but the peak position corresponds to the $8T_2$ state. In the Fernandez theoretical spectrum, no peaks were calculated for the second broad peak, probably because of the lack of the Rydberg basis set in the calculations.

The above quick overview of the SAC-CI study of the excitation spectra of metal complexes show the applicability, reliability, and usefulness of the SAC-CI method. Actually, these calculations are now small and easy ones in comparison with our recent calculations on porphyrins, for example.

11. Photochemical reactions and dynamics

Since the SAC method is a single reference theory, the SAC SD method is not applicable to quasi-degenerate electronic states which often appear in the dissociation of homolytic bonds. In

order that the SAC SD method is safely applicable, the HF configuration should be dominant throughout the process. Such cases are often found in isomerization processes, ionic dissociation processes, and van der Waals interactions, and for them we can calculate the potential curves of the ground, excited, ionized and electron attached states throughout the processes. The SAC/SAC-CI gradient technique should be useful for studying the dynamics involving the ground, excited, ionized and electronic attached states of a molecule and the coding has been finished very recently in our laboratory.

We show here, in some detail, the study of the collision-induced absorption spectra of the CsXe system, which is a typical van der Waals system.

11.1. Collision-induced absorption spectra of CsXe system

The optical S-S and S-D transitions of alkali atoms are dipole forbidden. However, when noble gas is admitted into alkali vapor, collisional interaction between alkali atom and noble gas makes these transitions dipole-allowed and new absorption bands are observed near the position of the originally forbidden line.[137] This phenomena is called collision-induced absorption. The position and the profile of the collision-induced absorption sensitively reflect the interatomic potentials of the ground and excited states of the alkali-noble gas system and the (induced) transition moments between them. We were very interested in this aspect of the collision-induced absorption. Moe et al. [137] reported the detailed absorption spectra for the Cs-noble gas systems.

We explain here our studies[69,70] on the collision induced absorption spectra of Cs-Xe. This system shows relatively strong interactions and its spectra represent most of the features common to the alkali-noble gas systems. We are interested in the Cs-Xe interactions in a relatively shorter region ($R_{Cs\text{-}Xe}$ < 10Å), so-called wing region where the van der Waals interactions, overlap interactions, and repulsive interactions cooperatively determine the interatomic potentials. Since the spectral profiles depend very sensitively on the potential energy curves of the ground and excited states and on the induced transition dipole moments between them, we need a theory which is able to describe both ground and excited states in a considerable accuracy.

As such a theory, we use the SAC/SAC-CI theory. A proper choice of the basis set is quite important for obtaining reliable results particularly for the excited states. In the first calculations,[69] we used the relativistic ECP and the basis set of Wadt and Hay[138] augmented with the diffuse functions presented by Langhoff et al.[139] However, we could not reproduce the proper ordering of the 5D and 7S states of the Cs atom, which is quite important for correctly reproducing the collision-induced spectra. In the refined calculations, we used the all-electron basis set of Huzinaga et al.,[140] after examining whether the reasonably correct result is obtained with this basis set for the excitation spectrum of the Cs atom. The basis set of Cs is composed of [7s5p2d] set for the valence part and augmented with the primitive (3s3p3d) set of Langhoff et al.[139] for the Rydberg part. The Xe basis set is [6s5p2d] set of Huzinaga[140] augmented with the primitives (3s2p) of Ermler et al.[141] The basis set superposition error (BSSE) was also taken into account in a usual way.

The quasistatic approximation[142] is adopted for calculating the reduced absorption coefficients. This approximation seems to be reliable and useful for understanding the mechanism of the collision-induced absorption process. Assuming binary collision between Cs and Xe atoms in the canonical distribution, the reduced absorption coefficient is given by

$$\frac{k(\lambda)}{n_G n_A} = \sum_c \frac{4\pi^3}{3\lambda} D(R_c)^2 \left(\frac{4\pi R_c^2}{d\left[V_e(R) - V_g(R)\right]/dR\Big|_{R_c}} \right) \exp\left(-\frac{V_g(R_c) - V_g(R_\infty)}{k_B T} \right), \tag{59}$$

where n_G and n_A are the densities of the perturber Xe and the absorber Cs, respectively, *D(R)* denotes the induced transition dipole moment at internuclear distance R, and V_g and V_e are the energies of the ground and excited states, respectively.

Thus, the collision induced absorption spectra are determined by the following three quantities, (1) excitation energies, (2) Boltzmann distribution of the ground state, and (3) induced transition moments, as the functions of the internuclear distance.

Figure 7 shows the calculated potential curves of the 6S, 6P, 5D, and 7S states of CsXe. The calculated potential curve of the ground state of CsXe has a flat shape with a shallow minimum of 30 cm^{-1} at 4.97 Å in comparison with the experimental values of 110 cm^{-1} at 5.45 Å.

The 6pΣ and 5dΣ states are due to the excitations from the 6s non-bonding MO to the weakly anti-bonding 6pσ and 5dσ MO's, so that the system becomes unstable and the potential curves are repulsive. The repulsive interaction in the 5dΣ state seems to be larger than that in the 6pΣ state, starting from a larger internuclear distance. The 5dΣ state has a characteristic hump at 4.6 Å and the 6pΣ state has a shoulder at 5.0 Å. The hump of the 5dΣ state is caused by the avoided crossing with the 7sΣ state, so that the natures of these states are reversed at this point, though in Figure 7 the upper curve is still called 7sΣ state and the lower one 5dΣ state even in the shorter region.

The 6pΠ, 5dΠ, and 5dΔ states have shallow minima in their potential curves. The Rydberg orbitals of these states of the Cs atom are not directed towards the rare gas atom, but the ion core of the Cs atom polarizes the electron density of the rare gas atom, which is responsible for the attractive force. The potential curve of the 7sΣ state also has a well at 4.61 Å which is due to the avoided crossing with the 5dΣ state, as noted above. The calculated spectroscopic constants were compared in ref. [70] with the experimental values.

From the potential curves shown in Figure 7, the excitation energies of the various states as functions of the internuclear distances are calculated. Figure 8 shows the Boltzmann distribution of the ground state as a function of the internuclear distance. Because of the repulsive nature of the potential curve in the shorter region than 4.5 Å, the probability of finding the ground state in this region becomes very small.

The absolute values of the induced dipole moments are shown in Figure 9 as a function of the internuclear distance. These induced moments are mainly due to the intra-atomic orbital mixing of the p-component of the Cs atom, caused by a reduction of the spatial symmetry of the system. The

5dΔ state does not have an induced transition dipole moment and therefore gives no contribution to the induced absorption spectra.

The induced transition moment is an important factor, as seen from Eq. (59), in determining the intensity of the induced absorption. The 6sΣ-5dΣ transition moment is induced at larger internuclear distances than that of 6sΣ-7sΣ: the p-component of the Cs atom interacts more readily in the 5dΣ state than in the 7sΣ state. Since the Boltzmann factor of the ground state sharply decreases in the repulsive region, $R < 4$, this explains the observation that the intensity of 6sΣ-5dΣ are larger than those of 6sΣ-7sΣ. The magnitude of the transition moment is reversed between the 5dΣ and 7sΣ states at the avoided crossing point. The 6sΣ-7sΣ transition moment shows an oscillatory structure, reflecting the nodal property of the p-component mixed into the 7sΣ state. Due to this nodal property, the CsXe interaction at around 5 - 6 Å has only a small contribution to the collision induced absorption around the 7S line. The calculated transition moments seem to be underestimated in comparison with the experimental results as discussed below.

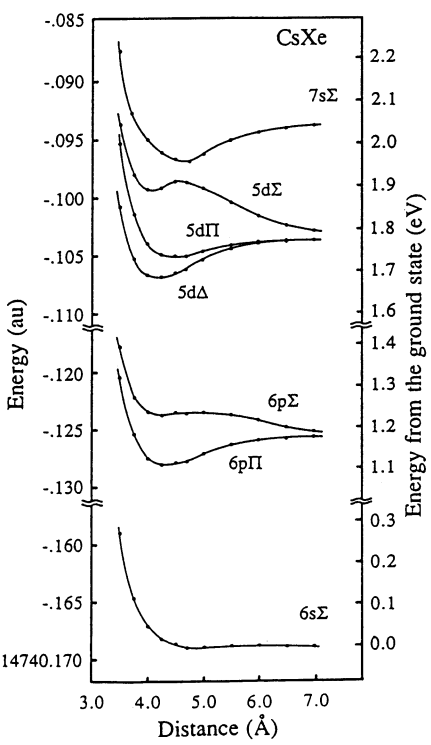

Figure 7: Potential energy curves of the 6s, 6p, 5d, and 7s states of the CsXe system without spin-orbit coupling.

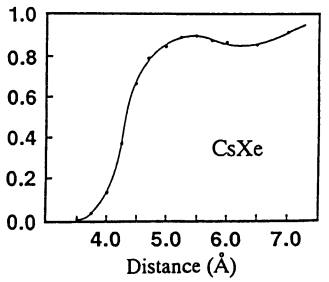

Figure 8: Boltzmann distribution function for the ground state of CsXe (T=371 °C).

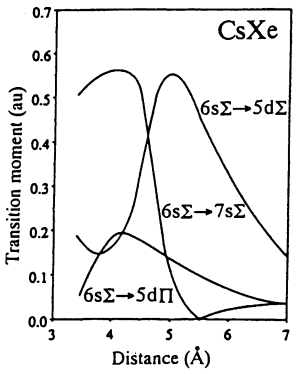

Figure 9: Absolute values of the transition dipole moments for the 6sΣ→ 5dΣ, 6sΣ→ 5dΠ, and 6sΣ→ 7sΣ transitions of the CsXe system.

The collision induced absorption spectra are calculated from the quasistatic approximation, Eq. (59) using the quantities given in Figures 7, 8, and 9. The calculated spectra associated with the 5D line are shown in Figure 10 together with the experimental one. The 6S-5D transition of the Cs atom is calculated at 697 nm in comparison with the experimental value of 692nm. The experimental peak in the blue side of this transition is attributed to the $6s\Sigma \rightarrow 5d\Sigma$ transition of the collision complex. In the theoretical spectra, R denotes, in the classical picture, the internuclear distance of the collision complex at which the absorption of the light of a given wavelength occurs.

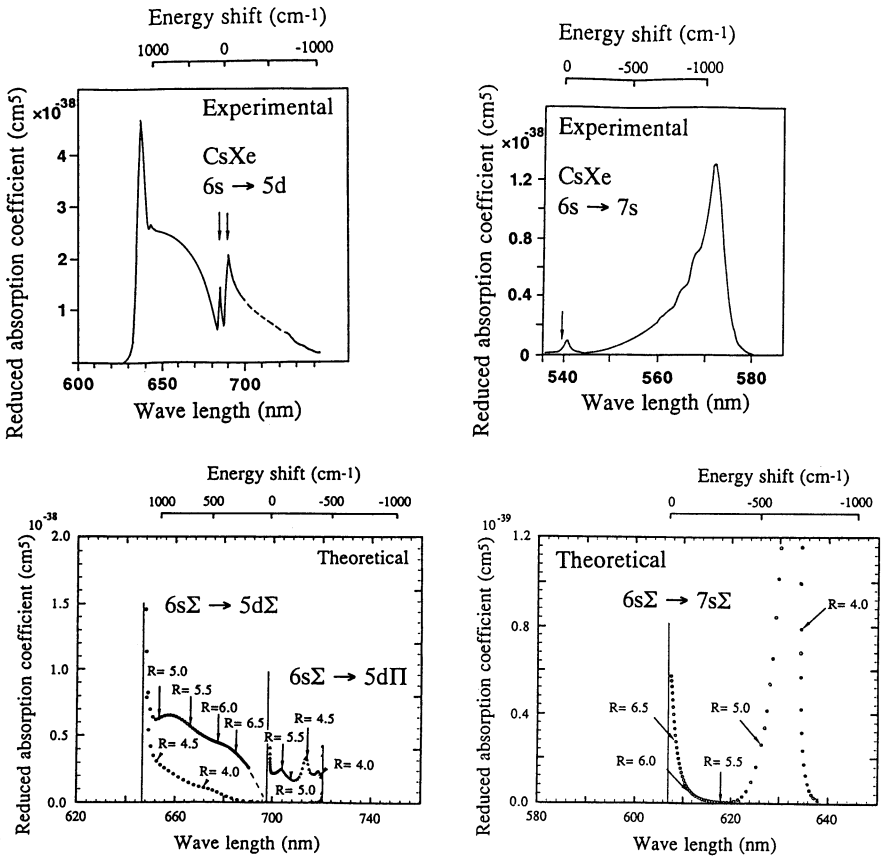

Figure 10: Reduced absorption coefficients for the 5d states of CsXe. The experimental spectra are due to Moe et al.,[137] and the SAC-CI theoretical spectra is from ours.[70]

Figure 11: Reduced absorption coefficients for the 7s states of CsXe. The experimental spectra are due to Moe et al.,[137] and the SAC-CI theoretical spectra is from ours.[70]

The theoretical curve shows that it is a sum of the two absorptions of the complex at different distances, R. The steep cusp exists in both experimental and theoretical spectra and is due to the extremum in the excitation energy dependence on R: in Eq. (59), the intensity diverges at this extremum. From the R-values in the theoretical spectrum and from the potential curves shown in Figure 7, we see that this extremum is due to the hump of the 5dΣ potential lying between 4.5 and 5.0Å. Namely, the cusp in the spectrum is assigned as being due to the hump of the 5dΣ potential.

Both experimental and theoretical spectra have shoulders on the right-hand-side of the cusp. From the theoretical spectra, we see that this shoulder is due to the absorptions in the region of R = 5 - 6 Å. From Figure 9, we see that this large intensity is due to the large transition dipole moment of the 6sΣ → 5dΣ transition in this region of R, which is due to the avoided crossing between the 5dΣ and 7sΣ sates. Namely, the shoulder of the 6sΣ → 5dΣ line is a proof of the avoided crossing between the 5dΣ and 7sΣ states in the 5 - 6 Å region.

The absorption band observed in the red side of the 6S-5D transition of Cs is due to the 6sΣ → 5dΠ transition of the collision complex. This transition is calculated to have smaller intensity than the 6sΣ → 5dΣ transition, in agreement with the experiment. Our theoretical transition has at least two peaks, due to the absorptions at R=5.5 and 4.5 Å, and vanishes at about 720 nm. However, experimentally, this transition is difficult to observe precisely because of the existence of the absorption band of Cs_2 in this region.

Figure 11 shows the collision induced absorption spectra owing to the 6sΣ → 7sΣ transition of the collision complex. The 6S-7S atomic line is calculated at 607 nm in comparison with 540 nm of the experimental spectrum. The induced absorption peak separated by about 30 nm in the experimental spectrum is reproduced in the theoretical one separated by 23 nm. This peak is due to the potential minimum of the 7sΣ state. The vibrational structure of the experimental spectrum indicates an existence of the attractive well in the excited state, which certainly exists in the potential curve shown in Figure 7.

Thus, from the present study of the collision induced absorption spectra, we could show that the spectral peaks, shoulders and shapes reflect the detailed behaviors and characters of the CsXe collision complex. Having such an understanding on the absorbed spectra, we can increase the insight about the nature of the collision dynamics and the formed complexes.

12. Excited states of porphyrins

Recently, the SAC-CI method has been applied to porphyrins to understand their electronic structures and the excited states. Porphyrins are key compounds in biology: there are rich chemistry and physics involving porphyrins. Porphyrins appear in many key biological processes. Therefore, correct understanding of their energy levels and electronic structures is quite important. For example, the excitation and electron transfer processes occurring in the photosynthetic reaction center are quite interesting subject from the quantum-chemical point of view. Furthermore, porphyrins are moderately large and moderately complex from the standpoint of the accurate ab initio computational method like SAC-CI, and therefore give nice challenging subjects. We study

porphyrin chemistry from the interests of both biological chemistry and computational chemistry. This is certainly a new trend fitting to the subject of this book.

12.1. Free base porphin

Our first SAC-CI calculations on porphyrins were done for free base porphin (FBP), $C_{20}N_4H_{14}$.[49] The geometry was assumed to have D_{2h} symmetry with D_{4h} skeleton. The basis set is valence p-double quality; Huzinaga's (63/5)/[2s2p] set for carbon and nitrogen and (4)/[1s] set for hydrogen. The total number of Hartree-Fock SCF MOs are 206. In the SAC/SAC-CI calculations, the active orbitals consist of 156 MOs, the higher 42 occupied and lower 114 unoccupied MOs. The number of the linked operators are reduced by using the configuration selection procedure.

Table 11 shows the HF orbitals of FBP. We see that the HOMO ($2a_u$) and the next HOMO ($5b_{1u}$) are quasi-degenerate and LUMO ($4b_{2g}$) and next LUMO ($4b_{3g}$) are almost degenerate. These four orbitals are well separated from the others, so that they play a crucial role in the lower excited states. The importance of these four orbitals was first notified by Gouterman in his 'four orbital' model.[143]

Table 11: HF orbital energy and orbital nature of porphin.

MO	orbital energy (eV)	character
Higher occupied orbitals		
$7a_g$	-14.661	σ
$6b_{2u}$	-14.646	σ
$7b_{3u}$	-14.480	σ
$7b_{1g}$	-14.355	σ
$1a_u$	-12.216	π
$7b_{2u}$	-11.415	n
$8a_g$	-11.263	n
$3b_{1u}$	-10.679	π
$2b_{2g}$	-10.632	π
$2b_{3g}$	-10.590	π
$3b_{2g}$	-10.321	π
$4b_{1u}$	-9.327	π
$3b_{3g}$	-9.122	π
$5b_{1u}$	-6.686	π
$2a_u$	-6.521	π
Lower unoccupied orbitals		
$4b_{2g}$	-0.069	π
$4b_{3g}$	0.141	π
$3a_u$	2.842	π
$6b_{1u}$	5.064	π
$5b_{2g}$	5.698	π
$5b_{3g}$	5.702	π
$4a_u$	6.177	π
$8b_{3u}$	6.852	σ
$8b_{2u}$	7.437	σ
$8b_{1g}$	8.046	σ

Table 12 summarizes the SAC-CI results for the excited states of FBP. It also gives the experimental excitation energy and the results of other ab initio calculations. Figure 12 shows the gas-phase experimental spectrum[144] compared with the SAC-CI result.

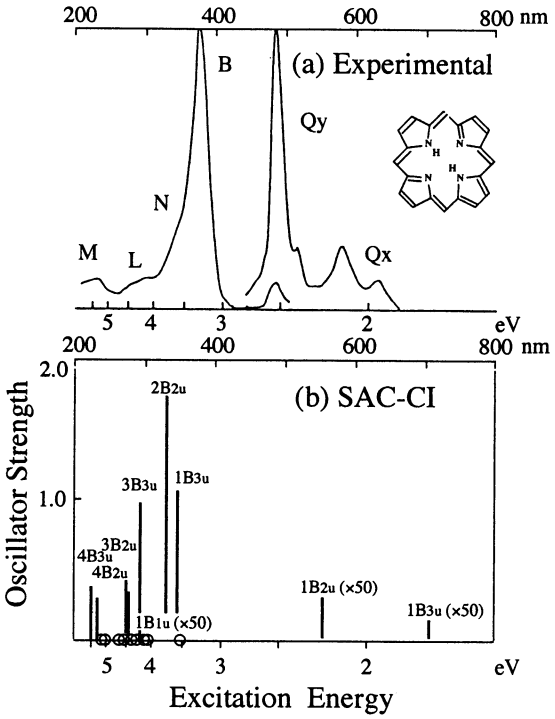

Figure 12: Electronic spectra of free base porphin. (a) Gas-phase experimental spectrum due to Edwards et al.[144] and (b) SAC-CI theoretical spectrum. The optically forbidden states are indicated by open circles.

In the previous ab initio studies, only the lower four states were reported.[145-148] Nagashima et al.[145] were the first who performed MRSDCI within the π-space. Though the results were not very satisfactory due to the smallness of the basis set and the active space, their calculation was certainly pioneering in those days and they clarified the essential features of the excited states of this molecule. Yamamoto et al.[147] further carried out MRSDCI using improved basis and including σ space: their results agree well with the experimental values. Foresman et al.[146] performed CIS calculations. More recently, Roos et al.[148] performed CASPT2 calculations: probably this was the best calculation performed on this molecule before SAC-CI was done. However, all of the previous calculations were limited only to the lower 4 states: this limitation may be good for the Q band but not for the B band, because our results show that the main configurations of the B band strongly

Table 12: Excited states of free base porphin calculated by the SAC-CI and other theoretical methods.

	SAC-CI					Exptl.[b]		Other ab initio theoretical excitation energy (eV)			
State[a]	Main configuration (C > 0.3) (eV)	Nature	Excitation energy (eV)	Polari-zation	Oscillator strength	Excitation energy (eV)		MRSDπCI[c]	CIS[d]	MRSDσπCI[e]	CASPT2F[f]
$1B_{3u}$	0.73 ($5b_{1u} \rightarrow 4b_{2g}$)-0.61 ($2a_u \rightarrow 4b_{3g}$)	π–π*	1.75	x	1.13×10^{-3}	1.98	Qx	2.27	2.53	1.97	1.70
$1B_{2u}$	-0.70 ($2a_u \rightarrow 4b_{2g}$)-0.66 ($5b_{1u} \rightarrow 4b_{3g}$)	π–π*	2.23	y	5.66×10^{-3}	2.42	Qy	3.42	2.66	2.40	2.26
$1B_{1g}$	0.93 ($3b_{3g} \rightarrow 4b_{2g}$)	π–π*	3.55		0.0						
$2B_{3u}$	-0.64 ($2a_u \rightarrow 4b_{3g}$)+0.52 ($4b_{1u} \rightarrow 4b_{2g}$) -0.43 ($5b_{1u} \rightarrow 4b_{2g}$)	π–π*	3.56	x	1.03	3.33	B	4.72 5.29	4.6 4.8	3.41 3.24	2.91 3.04
$2B_{2u}$	0.66 ($5b_{1u} \rightarrow 4b_{3g}$)-0.63 ($2a_u \rightarrow 4b_{2g}$) -0.25 ($4b_{1u} \rightarrow 4b_{3g}$)	π–π*	3.75	y	1.73	3.65	N				
$1B_{2g}$	0.94 ($8a_g \rightarrow 4b_{2g}$)	n–π*	4.05		0.0						
$1A_u$	-0.93 ($7b_{2u} \rightarrow 4b_{2g}$)	n–π*	4.18		0.0						
$3B_{3u}$	0.76 ($4b_{1u} \rightarrow 4b_{2g}$)+0.33 ($2a_u \rightarrow 4b_{3g}$) -0.40 ($5b_{1u} \rightarrow 4b_{2g}$)	π–π*	4.24	x	0.976	4.25	L				
$2A_g$	0.88 ($3b_{3g} \rightarrow 4b_{3g}$)-0.32 (2au → 3au)	π–π*	4.25		0.0						
$1B_{3g}$	0.94 ($8a_g \rightarrow 4b_{3g}$)	π–π*	4.37		0.0						
$1B_{1u}$	0.93 ($7b_{2u} \rightarrow 4b_{3g}$)	n–π*	4.51	z	5.30×10^{-3}		L				
$3B_{2u}$	0.89 ($4b_{1u} \rightarrow 4b_{3g}$)	π–π*	4.52	y	0.350	4.67	L				
$2B_{1g}$	0.91 ($2a_u \rightarrow 6b_{1u}$)	n–π*	4.62		0.0						
$3A_g$	-0.86 ($2a_u \rightarrow 3a_u$)-0.35 ($3b_{3g} \rightarrow 4b_{3g}$)	π–π*	4.74		0.0						
$3B_{1g}$	0.66 ($2b_{3g} \rightarrow 4b_{2g}$)+0.65 ($3b_{2g} \rightarrow 4b_{3g}$)	π–π*	5.13		0.0						
$4A_g$	0.86 ($3b_{2g} \rightarrow 4b_{2g}$)-0.31 ($2b_{3g} \rightarrow 4b_{3g}$)	π–π*	5.28		0.0						
$4B_{2u}$	0.90 ($3b_{1u} \rightarrow 4b_{3g}$)	π–π*	5.31	y	0.280	5.3	M				
$4B_{3u}$	-0.93 ($3b_{1u} \rightarrow 4b_{2g}$)	π–π*	5.45	x	0.351		M				

[a] Bold face letter is for the optically allowed state.
[b] Reference 144.
[c] Reference 145.
[d] Reference 146.
[e] Reference 147.
[f] Reference 148.

interact with those of the higher excited states: calculating both states adequately, letting them interact properly, is important.

The SAC-CI method is effective and straightforward, so that we need not to restrict only to the lower four excited states. Table 12 shows the SAC-CI result of not only the optically allowed states, but also the optically forbidden states below 5.5 eV. The optically allowed eight π-π^* and one n-π^* excited states and the dipole-forbidden six π-π^* and three n-π^* states were calculated. Main configurations, natures, excitation energies and oscillator strengths are also given.

Referring to Table 12 and Figure 12, we see that the present SAC-CI results reproduce well the experimental spectrum in both excitation energy and oscillator strength. The average discrepancy from the observed peaks is 0.14 eV.

The Q band is composed of the two weak peaks Q_x and Q_y at 1.98 and 2.42 eV, respectively, and Q_y has a larger intensity than Q_x. By the SAC-CI calculations, Q_x and Q_y are assigned to the $1B_{3u}$ and $1B_{2u}$ states calculated at 1.75 and 2.23 eV, respectively. No other excited states including forbidden states are found in this area. They are polarized in x and y directions, respectively, in consistent with the polarization experiment. The main configurations are composed of the excitations within 'four-orbitals': two configurations mix in a quasi-degenerate manner.

A strong B (Soret) peak and a shoulder N is observed in the higher energy side of the spectrum. The four-orbital model of porphin explained that the B band consists of the two degenerate states. In some previous theoretical studies,[145-148] the B band was assigned to the two nearly degenerate $2B_{3u}$ and $2B_{2u}$ states, and the N band was left unassgined. However, our SAC-CI results indicate different assignment. The excitation energies of the $2B_{3u}$ and $2B_{2u}$ states are calculated at 3.56 and 3.75 eV, respectively and no other peaks are calculated in the 3 ~ 4 eV region. Then, we assign the $2B_{3u}$ and $2B_{2u}$ states to the B and N bands, respectively. The calculated excitation energies are larger than the experimental values by 0.23 and 0.10 eV, respectively. The energy splitting between the B and N bands, which is 0.32 eV, is calculated to be 0.20 eV. Furthermore, if the conventional assignment is adopted, no assignment is possible for the N band. Namely, the present proposal for the B and N bands are based not only on the calculated excitation energies for the $2B_{2u}$ and $2B_{3u}$ states, but also on the comparison of our result, as a whole, with the peaks in the experimental spectrum. The present assignment is supported also by the following observations.

The main configurations of the $2B_{3u}$ and $2B_{2u}$ states shown in Table 12 include not only the excitations within the 'four-orbitals', but also the excitations from the lower $4b_{1u}$ orbital, which has a large amplitude on N's not bonded to H, and the extent of mixing is largely different between the $2B_{3u}$ and $2B_{2u}$ states, so that these states are no longer quasi-degenerate. The natures of the B ($2B_{3u}$) and N ($2B_{2u}$) bands are different in this point from that of the Q band. In the CASPT2F calculation, which give very close B_x and B_y states, the $4b_{1u}$ MO was not included in the active space of CASSCF, though as shown here it strongly perturbs the picture of the four orbital model of the B band.

The polarization studies for the free base tetraphenylporphin[149,150] showed that the sharp B band and the shoulder are polarized perpendicular to each other and have the same polarizations as the Q_x and Q_y peaks, respectively. This is consistent with our assignment.

Referring to Figure 12 and Table 12, we see that the calculated intensity is larger for the $2B_{2u}$ (N) states than for the $2B_{3u}$ (B) states. This may contradict with the observed spectrum shown in Figure 12. However, we may interpret the observed spectrum as follows. The N band is a broad band, the B band is sharp, and the B band lies on the right-hand side of the broad N band, so that the N band looks like a shoulder of the B band.

The effects of the σ electron-correlation were found to be important for the description of the π-π^* excitations of the π conjugated systems. We have pointed out this fact many years ago in the SAC-CI study of benzene.[89] It was also pointed out by CASPT2,[148,151-153] and other calculations[154-156] in particular for larger π-electron molecules. Our calculations show that the mixing of the σ–σ^* excitations is large for the B and N states, but small for the Q_x and Q_y states.

For the L and M bands, no ab initio calculations have been reported except for the semi-empirical treatments.[157,158] The L bands at 4.25 and 4.67 eV are assigned to the $3B_{3u}$ and $3B_{2u}$ states calculated at 4.24 and 4.52 eV, respectively, since these two states have relatively large intensities (for the $1B_{1u}$ state, see below). The polarizations of these states, including 1Blu, are all different, so that a detailed experimental study is interesting. Since the intensity of the $3B_{3u}$ state is larger than that of the $3B_{2u}$ state, the shape of the L band is unsymmetric with higher intensity in the lower energy side in agreement with experiment. The main configurations of the $3B_{3u}$ and $3B_{2u}$ states are the transitions from the $4b_{1u}$ MO to the $4b_{2g}$ and $4b_{3g}$ MOs, respectively, which are the mixing configurations to the four orbital model in the B and N bands. Therefore, it is necessary to describe all these states in the same approximation.

It is interesting to note that we have obtained several n-π^* transitions. Among these, the optically allowed one is the $1B_{1u}$ state calculated at 4.5 eV, but the calculated intensity is very small. In the experimental spectrum, this peak may be concealed by the L band. Since the $7b_{2u}$ MO is the lone pair orbital on nitrogen, it will be blocked by forming metal porphyrins, so that this peak will disappear. We have obtained several other n-π^* states at 4.05 ~ 4.37 eV, but they are all optically forbidden.

The M band at around 5.3 eV in the experimental spectrum is composed of the two π-π^* transitions due to the $4B_{2u}$ and $4B_{3u}$ states. They are the transitions from the $3b_{1u}$ MO to the $4b_{3g}$ and $4b_{2g}$ MOs, respectively. In comparison with the L band, the starting MO is lower but the ending MOs are the same. Note that the order of the polarizations is different: x and y in the increasing energy for the L band and y and x for the M band. Experimental examination of such polarization property is also interesting.

12.2. Tetrazaporphin

Free base tetrazaporphin (FBTAP) (also called porphyrazine or tetraazaporphyrin) $C_{16}N_8H_{10}$ is a tetraaza-derivative of porphin. Phthalocyanine, which is a much more popular compound, is

regarded as a tetrabenzo-derivative of TBTAP. Science of porphins and phthalocyanines have a rich accumulation, while tetrazaporphins have been left out of the interest for a long time. In the past, FBTAP is mainly considered as a model compound of phthalocyanine, especially in theoretical studies. Phthalocyanines have intense absorption bands in the visible region, so that they are used as commercial pigments. Since FBTAP has similar intense bands in the visible region (so called Q bands), it is important to clarify the reason why FBTAP has such intense Q bands, in contrast to FBP studied above.

We review here the SAC/SAC-CI calculations of the ground and excited states of FBTAP,[114] which was the first ab initio study of the excited states of FBTAP. The basis set is of double-ζ quality for the valence 2p orbitals and then the SCF MOs consist of 81 occupied and 121 unoccupied MOs. In the SAC/SAC-CI calculations, only the 1s core orbitals of carbons and nitrogens were frozen; the higher 57 occupied and 121 all unoccupied MOs were included in the active space. The total number of active orbitals is 178.

Figure 13 is an illustration of the four orbitals in the HOMO-LUMO region and the two lower MOs. The energy levels of these MOs are shown in Figure 14, together with those of the free base

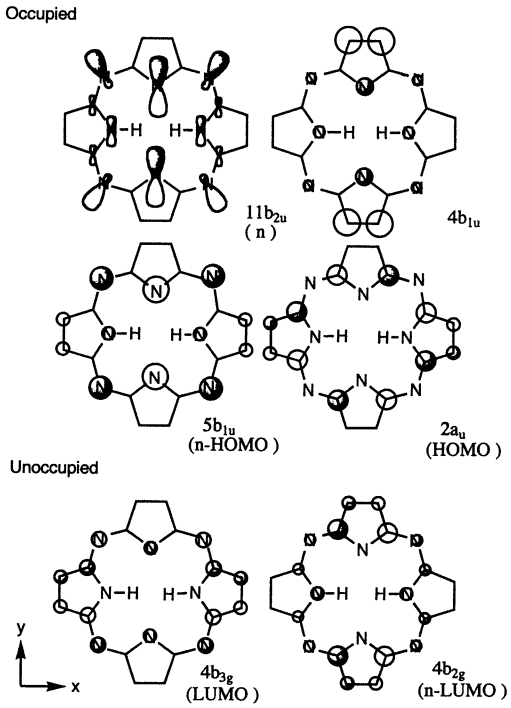

Figure 13: Occupied and unoccupied orbitals of FBTAP. All MOs have π character except for the $11b_{2u}$ orbital, which is n orbital.

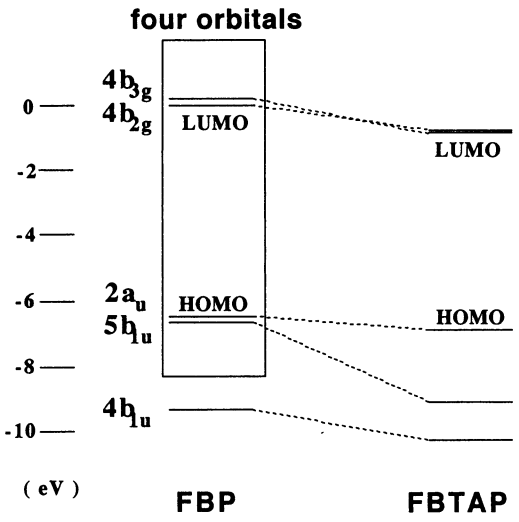

Figure 14: Orbital energies of the four orbitals and the lower $4b_{1u}$ MO of FBP and FBTAP.

porphin (FBP) for comparison. The ordering of two LUMOs is different, but they are almost degenerate. What is prominently different is the energy level of the $5b_{1u}$ MO. This MO has large amplitudes on the meso nitrogens, so that it is much lowered in FBTAP. Namely, the quasi-degeneracy of the two HOMOs in FBP is destroyed in FBTAP, which leads to the breakdown of the four orbital model in FBTAP. The next lower b_{1u} orbital, $4b_{1u}$ MO is the MO which mixes strongly in the main configurations of the B band of FBP.

Table 13 summarizes the excited states of FBTAP calculated by the SAC-CI method. The electronic spectra of FBTAP are shown in Figure 15. The upper one is experimental,[159] and the lower one is the SAC-CI theoretical spectrum. The most important feature of the FBTAP spectrum is that the Q bands have much larger intensities than those of FBP. The observed intensity ratio of the Q band/B band is 0.02 for FBP in benzene but 0.9 for FBTAP in chlorobenzene.

The Q band is composed of the two strong peaks Q_x and Q_y at 2.01 and 2.27 eV, respectively. By the SAC-CI calculations, Q_x and Q_y are assigned to the $1B_{3u}$ and $1B_{2u}$ states calculated at 1.88 and 2.26 eV, respectively. No other allowed excited states are found in this region. The error in the excitation energy is within 0.13 eV. The oscillator strengths of the Q_x and Q_y bands are calculated to be 0.152 and 0.220, respectively, which are quite large in comparison with those of FBP, 1.13×10^{-3} for Q_x and 5.66×10^{-3} for Q_y. The $1B_{3u}$ and $1B_{2u}$ states are polarized in the x and y directions, respectively (the x axis is along the N-H H-N bonds), in agreement with the experiment.

Table 13: Excited states of FBTAP calculated by the SAC-CI method

State	Main cofiguration ($C \geq 0.30$)	Nature	Excitation energy (eV)	Polarization	Oscillator strength	Exptl. Excitation energy (eV)	
	SAC-CI						
$1B_{3u}(Q_x)$	$0.79(2a_u \rightarrow 4b_{3g})-0.54(5b_{1u} \rightarrow 4b_{2g})$	$\pi \rightarrow \pi^*$	1.88	x	0.152	2.01	Q_x
$1B_{2u}(Q_y)$	$0.83(2a_u \rightarrow 4b_{2g})+0.47(5b_{1u} \rightarrow 4b_{3g})$	$\pi \rightarrow \pi^*$	2.26	y	0.220	2.27	Q_y
$2B_{3u}(B_x)$	$-0.63(4b_{1u} \rightarrow 4b_{2g})-0.56(5b_{1u} \rightarrow 4b_{2g})$ $-0.41(2a_u \rightarrow 4b_{3g})$	$\pi \rightarrow \pi^*$	3.56	x	0.500	3.3	
$1B_{1u}$	$-0.86(11b_{2u} \rightarrow 4b_{3g})+0.32(11b_{3u} \rightarrow 4b_{2g})$	$n \rightarrow \pi^*$	3.81	z	0.016		
$2B_{2u}(B_y)$	$-0.73(5b_{1u} \rightarrow 4b_{3g})-0.47(4b_{1u} \rightarrow 4b_{3g})$ $+0.37(2a_u \rightarrow 4b_{2g})$	$\pi \rightarrow \pi^*$	3.93	y	0.804	3.72	B
$2A_g$	$0.93(3b_{3g} \rightarrow 4b_{3g})$	$\pi \rightarrow \pi^*$	4.26		forbidden		
$3B_{2u}$	$-0.70(3b_{1u} \rightarrow 4b_{3g})+0.57(4b_{1u} \rightarrow 4b_{3g})$	$\pi \rightarrow \pi^*$	4.32	y	0.412		
$3B_{3u}$	$0.66(4b_{1u} \rightarrow 4b_{2g})-0.44(3b_{1u} \rightarrow 4b_{2g})$ $-0.43(5b_{1u} \rightarrow 4b_{2g})-0.31(2a_u \rightarrow 4b_{3g})$	$\pi \rightarrow \pi^*$	4.52	x	1.091		
$4B_{2u}$	$-0.61(3b_{1u} \rightarrow 4b_{3g})-0.59(4b_{1u} \rightarrow 4b_{3g})$ $+0.38(5b_{1u} \rightarrow 4b_{3g})$	$\pi \rightarrow \pi^*$	4.93	y	1.056		
$4B_{3u}$	$0.83(3b_{1u} \rightarrow 4b_{2g})-0.34(5b_{1u} \rightarrow 4b_{2g})$	$\pi \rightarrow \pi^*$	5.09	x	0.816		

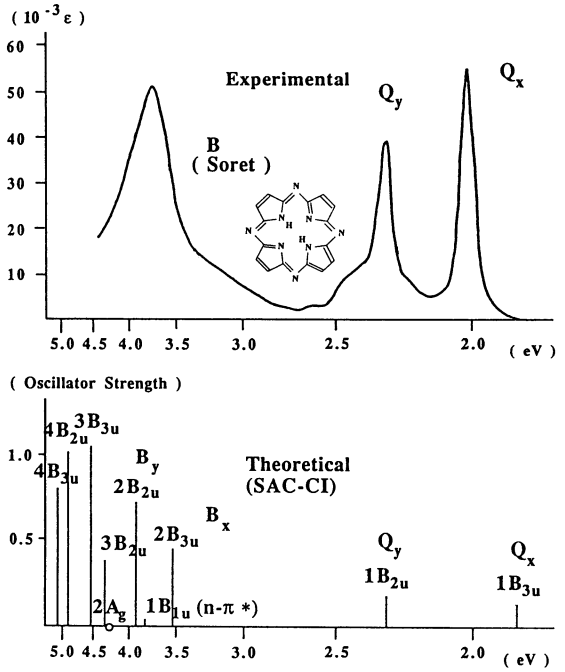

Figure 15: Electronic excitation spectra of FBTAP observed in chlorobenzene[159] and calculated by the SAC-CI method. The optically forbidden $2A_g$ state is indicated by the open circle.

Now, why are the intensities of the Q bands so strong in contrast to those of FBP? This point is important since it is related with the reason why phthalocyanines are useful as pigments. In both FBP and FBTAP, the Q band is written by a superposition of two configurations. For example, the $1B_{2u}$ state representing the Q_y band is written by a superposition of the two configurations, $2a_u \rightarrow 4b_{2g}$ and $5b_{1u} \rightarrow 4b_{3g}$, as shown in Table 13. In FBP, the absolute values of the coefficients of the two main configurations are approximately equal (*e.g.*, 0.70 and 0.66 for Q_y) reflecting the validity of the four orbital model. The transition dipole moment is expressed by a sign-reversed superposition of these two configurations, and therefore, when the weights of the configurations are equal, the moment is canceled out. This is why the Q band of FBP is weak. On the other hand, in FBTAP, the coefficients of the two main configurations in the Q band are unbalanced by the lowering of the $5b_{1u}$ MO. For example, the Q_y band of FBTAP consists of the superior (0.83) ($2a_u \rightarrow 4b_{2g}$) and the inferior (0.47) ($5b_{1u} \rightarrow 4b_{3g}$) configurations, because the energy difference between $2a_u$ and $4b_{2g}$ is smaller than that between $5b_{1u}$ and $4b_{3g}$. This unbalanced superposition of the configurations results in a large net transition moment. In ref. [114], this situation was explained using an illustrative diagram.

Thus, the strong intensity of the Q band of FBTAP is due to the breakdown of the four orbital model by the lowering of the next-HOMO which is localized on the meso nitrogens.

The Q band is in the visible region, therefore its strong intensity colors the molecule. In fact, a solution of FBTAP is violet-blue for transmitted light. Phthalocyanines, which have a common skeleton to FBTAP, are widely used as pigments due to their intense Q bands.

We have shown recently[116] by the SAC-CI calculation of phthalocyanine that the reason of the strong Q band of phthalocyanine is two-fold. One is the meso-N substitution, likewise in FBTAP, and the other is the tetra-benzo substitution to FBTAP which leads to the four outer benzene rings. Though we can not explain here in detail for the lack of space, two effects are cooperative to increase the intensity of the Q band. For more details, see ref. [116].

The B band of FBTAP is strong and broad; Dvornikov et al. suggested that the band may include some overlapping components.[160] The present SAC-CI study reveals that three allowed transitions exist in this area. The $2B_{3u}$, $1B_{1u}$, and $2B_{2u}$ states are calculated at 3.56, 3.81, and 3.93 eV, respectively. The $2B_{3u}$ (B_x) state is polarized in the x direction, and its oscillator strength is calculated to be 0.500. It would correspond to the shoulder at around 3.3 eV on the right-hand side of the main peak. The $1B_{1u}$ state is the first n-π^* transition and polarized in the out-of-plane z direction. This is a weak transition, whose oscillator strength is calculated to be 0.016. The $2B_{2u}$ (B_y) transition is polarized in the y direction, and its oscillator strength is the largest of the three allowed transitions in the B band, namely 0.804; it would correspond to the main peak lying at 3.72 eV.

Dvornikov et al. observed the fluorescence polarization spectrum of FBTAP[160] and showed that the B band was composed of a superposition of the transitions polarized in the x and y directions. They further proposed two possibilities that the y-component is predominant in the whole region from 2.95 to 4.13 eV and that the out-of-plane z-component exists. The present study

elucidates the existence of both x- and y-components, the predominance of the y-component, and the existence of the z-component, supporting the conjecture of Dvornikov et al.

The B_x band in the lower energy side has a smaller intensity than the B_y band in the higher energy side, which is supported by the experimental spectrum shown in Figure 15. Similar ordering of the intensities of the B_x and B_y bands was also seen in the SAC-CI result of FBP shown in the preceding section.

In FBP[144] the first allowed n-π^* transition was calculated as one component of the L bands, which lie higher than the B band. In FBTAP, the first allowed n-π^* transition appears relatively low and included in the B band. This n-π^* state consists of the major contribution representing the transition from the pyrrole N lone pair orbital and the minor contribution representing the transition from the meso N lone pair orbital. Such an interaction between the meso and pyrrole nitrogen lone pairs makes the n-π^* state stabilized in FBTAP.

In higher energy region of the B band, no experimental spectrum is reported. However, we calculated other four allowed transitions in this energy region; $3B_{2u}$, $3B_{3u}$, $4B_{2u}$, and $4B_{3u}$ excited states calculated at 4.32, 4.52, 4.93, and 5.09 eV, respectively. Since large oscillator strengths are calculated for these transitions, 0.412, 1.091, 1.056, and 0.816, respectively, we predict an existence of the intense bands in this area. Actually, for phthalocyanines the absorption spectra were observed beyond 4 eV, and the strong L and C bands were reported.[161] In FBP, we also obtained similar bands beyond the B and N bands, but the intensities were smaller there, and they were assigned to the relatively weak L and M bands of the experimental absorption spectrum.[49]

12.3. Carboxyheme and oxyheme

Hemoglobin and myoglobin play an important role in mammalian life through the transport and the storage of oxygen. Iron-porphyrin complex, called heme, constitutes their reaction center. In oxyheme, oxygen is at the distal site and imidazole is at the proximal site, while in carboxyheme, CO is replaced with O_2 of oxyheme. A poisoning molecule CO binds to iron porphyrin much more strongly than O_2.

We have studied the ground and excited states of oxyheme[113] and carboxyheme[115] using the SAC/SAC-CI method. We here introduce mainly the result on carboxyheme, and for oxyheme, we refer to ref. [113].

Carboxyheme, $FeC_{24}N_6OH_{16}$, consists of 48 atoms and 236 electrons, and its geometry is assumed to have Cs symmetry as shown in Figure 16. Note that the Fe-C1 bond deviates from the normal line of the porphyrin ring by 6° and the Fe-C1-O1 angle is 170°.

The quality of the GTO basis functions used is the same as those used previously for the calculations of porphyrins.[49,112-116] For the Fe atom, we use the Huzinaga's (5333/53/5)/[53321/53/41] set[140] plus p-type polarization function (0.082), for C, N, and O, the (63/5)/[63/41] set plus p-type anion basis (0.059) for oxygen, and for H the (4)/[4] set.[162] The basis set for imidazole is minimal; for C and N, the (63/5)/[63/5] set and for the H (4)/[4] set. The total number of the contracted GTOs is 278.

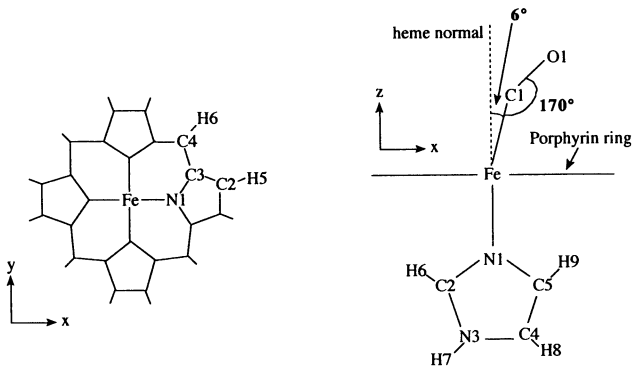

Figure 16: Geometry of carboxyheme.

In the SAC/SAC-CI calculations a total of 229 MOs were used as active MOs: all valence orbitals were included in the active space and only the 1s orbitals of C, N, and O atoms and the core orbitals (1s ~ 3p) of Fe were treated as frozen cores. All the single excitations and the selected double excitations within this active space constitute the linked operators and their products the unlinked operators. The perturbative configuration selection procedure was performed to reduce the size of the matrices involved in the calculations.

The Hartree-Fock orbitals of carboxyheme imply the validity of the four orbital model. Namely, the HOMO, next-HOMO, LUMO, and next-LUMO were well separated from the other MOs. These MO's are mainly porphyrin π-type, though some mixing of the Fe $d\pi$ orbitals is observed for the LUMO and next-LUMO. The HOMO is a_{1u} like MO and the next-HOMO is a_{2u} like in agreement with experiments.[163-166] The orbitals of the CO ligand do not appear in the HOMO-LUMO region. This is different from oxyheme. In oxyheme, LUMO was the orbital localized on Fe and O_2 and characterized not only the biological activity but also some aspect of the excitation spectrum of oxyheme.[167] In some lower occupied space, there exist the MOs that delocalize over the entire molecule, porphin ring, Fe, CO, and imidazole.

We calculated the excited states of carboxyheme in a wide energy range from visible to UV region, up to 7.8 eV, but the experimental spectrum[167] covers only up to 4.9 eV.

Figure 17 shows the electronic absorption spectrum of carboxyheme observed for the horse carboxyhemoglobin[167] compared with the excitation spectrum calculated by the SAC-CI theory in the UV and visible energy region, and Table 14 gives more detailed information on the excited states. The calculated spectrum well reproduces the experimental one in both the excitation energy and the oscillator strength, though horse carboxyhemoglobin is much different from the carboxyheme molecule calculated here. The first and second absorption peaks called Q_0 and Q_v bands are assigned to the 1A' and 1A" states, respectively. These Q bands are well described, as seen from Table 14, within the 'four orbital' model, and the calculated intensities are very small by the reason clarified in the previous section. In oxyheme, however, the Fe-O_2 π antibonding orbital,

which is LUMO, affects the nature of the Q bands.[113] Further, a weak band was observed in th spectrum of horse oxyhemoglobin at 1.34 eV in a lower energy region of the Q band:[167] it wa assigned by the SAC-CI calculations as being due to the excitation within the O_2 ligand.[113]

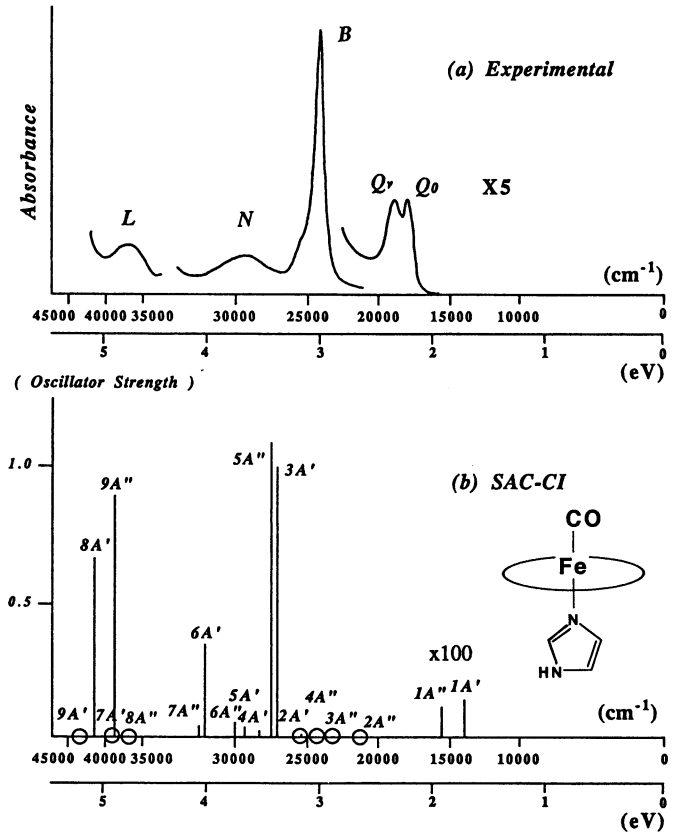

Figure 17: Electronic absorption spectra of carboxyheme. (a) Experimental spectrum of horsehemoglobin.[167] (b) SAC-CI theoretical spectrum. Open circles indicate singlet states with small oscillator strengths.

The B (Soret) band of carboxyheme is observed at around 3 eV of the experimental spectrum and it is assigned to the 3A' and 5A" states calculated at 3.36 and 3.41 eV with the large oscillator strengths of 1.04 and 1.13, respectively. These two peaks would explain the main peak and the shoulder at the higher energy side. Theoretically this shoulder corresponds to the N band of FBP, which also appears as a shoulder of the B band. We see again that the lower porphyrin π orbitals (MOs 74 and 73) mix into the B bands.

Table 14: Excited states of carboxyheme calculated by the SAC-CI method.

	SAC-CI					Exptl.[c]	
State	Main configuration [a] (|C|>0.25)	Nature [b]	Excitetion energy (eV)	Polari-zation	Oscillator strength	Excitation energy (eV)	
1A'	-0.77(77 - 80)+0.65(78 - 79)	π - π*	1.84	x	0.00139	2.18	Q_0
1A"	0.70(77 - 79)+0.65(78 - 80)	π - π*	1.94	y	0.00110	2.30	Q_v
2A"	-0.86(75 - 79)-0.27(63 - 79)	π - π*	2.72	y	0.00144		
3A"	0.55(76 - 80)+0.47(68 - 102) +0.42(69 - 108)+0.23(68 - 115)	d,π,σ - d*,π*,σ*	2.96	y	0.00037		
4A"	-0.68(76 - 80)+0.40(68 - 102) +0.36(68 - 108)	π - π*	3.00	y	0.00003		
2A'	0.64(75 - 80)-0.58(76 - 79)	π - π*	3.15	x	0.00742		
3A'	0.65(78 - 79)+0.51(77 - 80) -0.34(74 - 80)+0.26(73 - 80)	π - π*	3.36	x	1.04	2.96	B
5A"	0.66(78 - 80)-0.53(77 - 79) -0.39(73 - 79)	π - π*	3.41	y	1.13	2.96	B
4A'	0.64(76 - 79)+0.59(75 - 80)	π - π*	3.52	x	0.0179		
5A'	-0.46(63 - 101)+0.28(63 - 113) -0.27(75 - 101)-0.25(63 - 112)	d,σ - d*,σ*,CO*	3.63	x	0.0359		
6A"	0.39(62 - 101)-0.32(69 - 101) +0.29(76 - 101)-0.27(64 - 101)	d,σ - d*,σ*,CO*	3.72	y	0.0544		
6A'	-0.85(74 - 80)-0.35(77 - 80)	π - π*	3.98	x	0.350	3.60	N
7A"	-0.86(74 - 79)-0.35(73 - 79)	π - π*	4.06	y	0.0397		
8A"	-0.72(68 - 101)+0.34(68 - 113) -0.29(68 - 105)	d,σ - d*,σ*,CO*	4.65	y	0.00043		
9A"	-0.77(73 - 79)+0.39(74 - 79) +0.33(77 - 79)	π - π*	4.71	y	0.928	4.53	L
7A'	-0.93(78 - 81)	π - π*	5.01	x	0.00549		
8A'	0.91(73 - 80)	π - π*	5.12	x	0.655		M

[a] For MOs shown in the parentheses, see ref. 115.
[b] "σ" and "π" denote porphyrin σ and π MOs, respectively. "d" denotes Fe d orbital and "CO" the CO π antibonding orbital.
[c] Reference 167

The 4A', 5A', and 6A" states, which have small intensities, would exist near this shoulder and the N band. The 5A' and 6A" states have d,σ to d*,σ*,CO* nature (CO* is C-O π antibonding), so that these excited states may be connected with the photodissociation of CO in flashphotolysis experiments.[168-170]

The next strong band, called N band is assigned to the 6A' state. It originates from the excitation from the MO lower than the four orbitals and mixing into the B band. The nature of this state is just similar to the L band of FBP as seen from Tables 12 and 14.

The L band denoted in the experimental spectrum is assigned to the 9A" state. The nature of this state is also similar to that of the 6A' state: the excitation from the MO still lower is the main configuration. This state corresponds to the M band of FBP shown in Table 12. The 8A' state calculated at 5.12 eV also corresponds to the M band of the FBP. Thus, we conclude that the naming of the experimental band is different between FBP and carboxyheme.

In our calculations, the excited states lying higher than 5.2 eV were also calculated and given in ref [115]. The SAC-CI method is quite straightforward, so that there are no limitations for the number of states to be calculated. The natures of the excited states were very different from those

for the states lower than 5.2 eV. The main configurations could not be written using the four orbitals plus some lower orbitals: they include excitations involving Fe d orbitals and CO π^* orbitals in addition to the porphyrin π, and π^* MOs. For this reason, the intensities of the transitions lying higher than 5.2 eV were small. We predict that no intense band exists in the region above the L(M) band.

13. Remarks

In this review on SAC-CI, some theoretical aspects and some recent topics of interest were explained. Though the essential part of the theory of SAC/SAC-CI was established in 1978, it is still actively growing up as a methodology for studying chemistry and physics involving many different electronic states. Our current code is probably the fourth version, but still far from complete. We have recently finished the SAC/SAC-CI gradient code[171] which should be useful for studying the dynamics involving many different electronic states. We have a lot of charming subjects and dreams in the future of this SAC/SAC-CI project. In this situation, a review is only a progress report, and it is happy if the readers can feel something growing up in future.

This review has concerned only with the SAC/SAC-CI method. Interesting generalizations of this method were already published as the EGWF (exponentially generated wave function) approach,[55] which includes MRSAC,[64,65] EGCI,[56,57] and M(multi-)EG/EX(excited)-MEG methods.[66] Coding of these methods was completed[67] and very accurate results were obtained.[56,57,64-66] These methods also have high potentiality but left undeveloped for the lack of man power mostly of myself.

I also could not explain the SAC-CI applications to many interesting subjects, particularly to catalysis, surface chemistry, and surface photochemistry. However, I will be able to summarize it in a forthcoming review article.[172] Readers may also refer to the previous reviews on SAC-CI,[8-13] however many were written in Japanese.

14. Acknowledgment

The author thanks my colleagues on SAC-CI for various aspects of activities. He also thanks Dr. M. Ehara without whose kind helps, preparation of this chapter would have been more difficult. The reseraches summarized here were supported by the Grans-in-Aid for Scientific Research from the Japanese Ministry of Education, Science, and Culture and by the New Energy and Industrial Technology Development Organization (NEDO).

References

1. H. Nakatsuji and K. Hirao, *Chem. Phys. Letters* **47** (1977) 569.
2. H. Nakatsuji and K. Hirao, *J. Chem. Phys.* **68** (1978) 2053.
3. H. Nakatsuji, *Chem. Phys. Letters* **59** (1978) 362.
4. H. Nakatsuji, *Chem. Phys. Letters* **67** (1979) 329.
5. H. Nakatsuji, *Chem. Phys. Letters* **67** (1979) 334.
6. H. Nakatsuji, *Chem. Phys. Letters* **177** (1991) 331.
7. H. Nakatsuji and M. Ehara, *J. Chem. Phys.* **98** (1993) 7179.
8. H. Nakatsuji, *Reports of the Data Processing Center of Kyoto University, Kouhou* 19 (1986) 290 (in Japanese); H. Nakatsuji, *Supercomputer Workshop Report*, No. 5, Institute for Molecular Science, 1986, p. 27 (in Japanese).
9. H. Nakatsuji, O. Kitao, and M. Komori, *Proceedings of the Workshop on "Aspects of Many-Body Effects in Molecules and Extended Systems"*, February 1-10, 1988, Calcutta, India, ed. by D. Mukherjee, Lecture Notes in Chemistry-50, (Springer-Verlag, Berlin, 1989) pp.101-122.; O. Kitao, M. Komori, and H. Nakatsuji, *Supercomputer Workshop Report*, No.6, Institute for Molecular Science, 1987, p.75 (in Japanese).
10. H. Nakatsuji, *Acta Chimica Hungarica, Models in Chemistry* **129** (1992) 719.
11. H. Nakatsuji and M. Ehara, *Institute of Organosynthetic Chemistry*, Lecture No. 6, 115 (1992) (in Japanese).
12. H. Nakatsuji and H. Nakai, *Institute of Organosynthetic Chemistry*, Lecture No. 8, 92 (1994) (in Japanese).
13. H. Nakatsuji, *Institute of Organosynthetic Chemistry*, Lecture No. 10, 68 (1996) (in Japanese).
14. H. Nakatsuji, Program System for SAC and SAC-CI Calculations. Program Library No. 146 (Y4/SAC) Data Processing Center of Kyoto University, 1985.
15. H. Nakatsuji, Program Library SAC85 (No. 1396) Computer Center of the Institute for Molecular Science, Okazaki, Japan, 1986.
16. H. Nakatsuji, M. Hada, H. Nakai, M. Ehara, O. Kitao, and J. Hasegawa, SAC/SAC-CI code, 1996 version.
17. J. E. Mayer and M. G. Mayer, *Statistical mechanics*, (Wiley, New York, 1940), Chap.13.
18. O. Sinanoglu, *J. Chem. Phys.* **36** (1962) 706; **36** (1962) 3198; *Adv. Chem. Phys.* **6** (1964) 315.
19. H. Primas, in *Modern quantum chemistry*, Istanbul lectures, edited by O. Sinanoglu, (Academic, New York, 1965), Part 2, p.45.
20. J. Cizek, *J. Chem. Phys.* **45** (1966) 4256; *Adv. Chem. Phys.* **14** (1969) 35.
21. J. Paldus, in *New horizons of quantum chemistry*, ed. by P. -O. Löwdin and B. Pullman, (Reidel, Dordrecht, 1983), p. 81.
22. P. -O. Löwdin, *Adv. Chem. Phys.* **2** (1959) 209.
23. I. Shavitt, in Modern theoretical chemistry, edited by H. F. Schaeffer III, (Plenum, New

York, 1977), Vol. 3. p. 189.
24. R. J. Buenker and S. D. Peyerimhoff, in *New horizons of quantum chemistry*, ed. by P. -O. Löwdin and B. Pullman, (Reidel, Dordrecht, 1983), p.31.
25. E. R. Davidson, *The world of quantum chemistry*, ed by R. Daudel and B. Pullman, (Reidel, Dordrecht, 1974).
26. D. J. Thouless, *Nucl. Phys.* **21** (1960) 225.
27. H. Sekino and R. J. Bartlett, *J. Chem. Phys.* **82** (1985) 4225.
28. K. Hirao and H. Nakatsuji, *Chem. Phys. Letters* **79** (1981) 292.
29. T. Yonezawa, H. Nakatsuji, T. Kawamura, and H. Kato, *Chem. Phys. Letters* **2** (1968) 454; T. Yonezawa, H. Nakatsuji, T. Kawamura, and H. Kato, *J. Chem. Phys.* **51** (1969) 669.
30. H. Nakatsuji, H. Kato, and T. Yonezawa, *J. Chem. Phys.* **51** (1969) 3175.
31. H. Nakatsuji, *J. Chem. Phys.* **59** (1973) 2586.
32. H. Nakatsuji and K. Hirao, *J. Chem. Phys.* **68** (1978) 4279.
33. K. Ohta, H. Nakatsuji, K. Hirao, and T. Yonezawa, *J. Chem. Phys.* **73** (1980) 1770.
34. K. Ohta, H. Nakatsuji, I. Maeda, and T. Yonezawa, *Chem. Phys.* **67** (1982) 49.
35. K. Ohta, H. Nakatsuji, H. Kubodera, and T. Shida, *Chem. Phys.* **76** (1983) 271.
36. H. Nakatsuji, K. Ohta, and T. Yonezawa, *J. Phys. Chem.* **87** (1983) 3068.
37. D. Feller and E. R. Davidson, *J. Chem. Phys.* **80** (1984) 1006; *Theor. Chim. Acta* **68** (1985) 57.
38. T. Momose, H. Nakatsuji, and T. Shida, *J. Chem. Phys.* **89** (1988) 4185.
39. H. Nakatsuji and M. Izawa, *J. Chem. Phys.* **91** (1989) 6205.
40. H. Nakatsuji, M. Ehara, and T. Momose, *J. Chem. Phys.* **100** (1994) 5821.
41. J. A. Pople, J. S. Binkley, and R. Seeger, *Int. J. Quantum Chem. Symp.* **10** (1976) 1; J. A. Pople, R. Seeger, and R. Krishnan, *Int. J. Quantum Chem. Symp.* **11** (1977) 149.
42. R. J. Bartlett and G. D. Purvis, *Int. J. Quantum Chem.* **14** (1978) 561.
43. O. Kitao and H. Nakatsuji, *Proc. Indian Acad. Sci.* **96** (1986) 155.
44. K. Hirao and H. Nakatsuji, *J. Comp. Phys.* **45** (1982) 246.
45. E. R. Davidson, *J. Comput. Phys.* **17** (1975) 87.
46. H. Nakatsuji, SAC/SAC-CI program, 1979, unpublished.
47. H. Nakatsuji, SAC/SAC-CI program, 1981, unpublished.
48. H. Nakatsuji, *Chem. Phys.* **75** (1983) 425.
49. H. Nakatsuji, J. Hasegawa, and M. Hada, *J. Chem. Phys.* **104** (1996) 2321.
50. H. Nakatsuji, J. Ushio, and T. Yonezawa, *Can. J. Chem.* **63** (1985) 1857.
51. K. Itoh, *Chem. Phys. Letters* **1** 235 (1967); K. Itoh, in *Magnetic Molecular Materials*, edited by D. Gatteschi *et al.* (Kluwer Academic Dordrecht, the Netherlands, 1991).
52. Y. Teki, T. Takui, K. Itoh, H. Iwamura, and K. Kobayasi, *J. Am. Chem. Soc.* **108** 2147 (1986); I. Fujita,Y. Teki, T. Takui, T. Kinoshita, K. Ito, F. Miko, Y. Sawaki, H. Iwamura, A. Izuoka, and T. Sugawara, *J. Am. Chem. Soc.* **112** 4074 (1990).

53. S. Huzinaga, *J. Chem. Phys.* **42** (1965) 1293; T. H. Dunning Jr., *J. Chem. Phys.* **53** (1970) 2823.
54. K. Hirao and Y. Hatano, *Chem. Phys. Letters* **100** (1983) 519; **111** (1984) 533; H. Nakatsuji, K. Hirao, and Y. Mizukami, *Chem. Phys. Letters* **179** (1991) 555.
55. H. Nakatsuji, *J. Chem. Phys.* **83** (1985) 5743.
56. H. Nakatsuji, *J. Chem. Phys.* **94** (1991) 6716.
57. H. Nakatsuji and M. Ehara, *J. Chem. Phys.* **99** (1993) 1952.
58. K. P. Huber and G. Herzberg, *Molecular spectra and molecular structures*, Vol. 4. Constants of diatomic molecules (Van Nostrand Reinhold, New York, 1979).
59. K. Kirby and B. Liu, *J. Chem. Phys.* **70** (1979) 893; M. Dupuis and B. Liu, *J. Chem. Phys.* **73** (1980) 337.
60. J. A. Nichols and J. Simons, *J. Chem. Phys.* **86** (1987) 6972.
61. W. P. Kraemer and B. O. Roos, *Chem. Phys.* **118** (1987) 345.
62. C. W. Bauschlicher Jr. and S. R. Langhoff, *J. Chem. Phys.* **87** (1987) 2919.
63. M. Ehara and H. Nakatsuji, unpublished.
64. H. Nakatsuji, *J. Chem. Phys.* **83** (1985) 713.
65. H. Nakatsuji, *Theoret. Chim. Acta* **71** (1987) 201.
66. H. Nakatsuji, *J. Chem. Phys.* **95** (1991) 4296.
67. H. Nakatsuji, Program System for the EGWF and EX-EGWF Methods Applied to Molecular Ground, Excited, Ionized, and Electron Attached States, 1990.
68. Y. Mizukami and H. Nakatsuji, *J. Chem. Phys.* **92** (1990) 6084.
69. H. Nakatsuji and M. Ehara, *Chem. Phys. Letters* **172** (1990) 261.
70. H. Nakatsuji and M. Ehara, *J. Chem. Phys.* **102** (1995) 6822.
71. H. Nakai and H. Nakatsuji, *J. Mol. Struc. (Theochem)* **311** (1994) 141; H. Nakai, Y. Ohmori, and H. Nakatsuji, *J. Phys. Chem.* **99** (1995) 8550.
72. M. Hada, Y. Imai, M. Hidaka, and H. Nakatsuji, *J. Chem. Phys.* **103** (1995) 6993.
73. H. Nakatsuji and H. Nakai, *Chem. Phys. Letters* **174** (1990) 283.
74. H. Nakatsuji and H. Nakai, *J. Chem. Phys.* **98** (1993) 2423.
75. H. Nakatsuji, R. Kuwano, H. Morita and H. Nakai, *J. Mol. Catalysis* **82** (1993) 96.
76. H. Nakatsuji, H. Morita, H. Nakai, Y. Murata, and K. Fukutani, *J. Chem. Phys.* **104** (1996) 714.
77. H. Nakatsuji and K. Hirao, *Intern. J. Quantum Chem.* **20** (1981) 1301.
78. H. Nakatsuji, K. Ohta, and K. Hirao, *J. Chem. Phys.* **75** (1981) 2952.
79. H. Nakatsuji and T. Yonezawa, *Chem. Phys. Letters* **87** (1982) 426.
80. H. Nakatsuji, *Chem. Phys.* **76** (1983) 283.
81. H. Nakatsuji, *Intern. J. Quantum Chem. Symp.* **17** (1983) 241.
82. H. Nakatsuji, *J. Chem. Phys.* **80** (1984) 3703.
83. K. Hirao, *J. Am. Chem. Soc.* **106** (1984) 6283.
84. K. Hirao, *J. Chem. Phys.* **79** (1983) 5000.

85. H. Nakatsuji, O. Kitao, and T. Yonezawa, *J. Chem. Phys.* **83** (1985) 723.
86. M. Terazima, S. Yamauchi, N. Hirota, O. Kitao, and H. Nakatsuji, *Chem. Phys.* **107** (1986) 81.
87. H. Nakatsuji and M. Hada, *J. Am. Chem. Soc.* **107** (1985) 8264;
88. H. Nakatsuji, M. Hada, and T. Yonezawa, *J. Am. Chem. Soc.* **109** (1987) 1902.
89. O. Kitao and H. Nakatsuji, *J. Chem. Phys.* **87** (1987) 1169.
90. H. Nakatsuji, M. Komori, and O. Kitao, *Chem. Phys. Letters* **142** (1987) 446.
91. O. Kitao and H. Nakatsuji, *Chem. Phys. Letters* **143** (1988) 528.
92. O. Kitao and H. Nakatsuji, *J. Chem. Phys.* **88** (1988) 4913.
93. H. Nakatsuji, Y. Matsuzaki, and T. Yonezawa, *J. Chem. Phys.* **88** (1988) 5759.
94. H. Nakatsuji and S. Saito, *J. Chem. Phys.* **93** (1990) 1865.
95. H. Nakatsuji and S. Saito, *Intern. J. Quantum Chem.* **39** (1991) 93.
96. T. Momose, M. Yamaguchi, T. Shida, *J. Chem. Phys.* **93** (1990) 7284.
97. L. B. Knight, B. W. Gregory, D. W. Hill, and C.A. Arrington, *J. Chem. Phys.* **94** (1991) 67.
98. T. Shida, T. Kato, T. Momose, and M. Matsushita, *J. Chem. Phys.* **95** (1991) 4275.
99. H. Nakai, Y. Ohmori, and H. Nakatsuji, *J. Chem. Phys.* **95** (1991) 8287.
100. H. Nakatsuji, M. Ehara, M. H. Palmer, and M. F. Guest, *J. Chem. Phys.* **97** (1992) 2561.
101. H. Nakatsuji and M. Izawa, *J. Chem. Phys.* **97** (1992) 435.
102. H. Nakatsuji and H. Nakai, *Chem. Phys. Letters* **197** (1992) 339.
103. H. Nakatsuji and Y. Fukunishi, *Intern. J. Quantum Chem.* **42** (1992) 1101.
104. K. Yasuda and H. Nakatsuji, *J. Chem. Phys.* **99** (1993) 1945.
105. S. Jitsuhiro, H. Nakai, M. Hada and H. Nakatsuji, *J. Chem. Phys.* **101** (1994) 1029.
106. H. Nakatsuji and M. Ehara, *J. Chem. Phys.* **101** (1994) 7658.
107. V. Galasso, *J. Chem. Phys.* **102** (1995) 7158.
108. K. Endo, M. Saikawa, M. Sugimoto, M. Hada, and H. Nakatsuji, *Bull. Chem. Soc. Jap.* **68** (1995) 1601.
109. K. Yasuda, N. Kishimoto, and H. Nakatsuji, *J. Phys. Chem.* **99** (1995) 12501.
110. J. Hasegawa, K. Toyota, M. Hada, H. Nakai and H. Nakatsuji, *Theoret. Chim. Acta* **92** (1995) 351.
111. V. Galasso, *J. Mol. Struct. (THEOCHEM)* **337** (1995) 249.
112. J. Hasegawa, M. Hada, M. Nonoguchi, and H. Nakatsuji, *Chem. Phys. Letters* **250** (1996) 159.
113. H. Nakatsuji, J. Hasegawa, H. Ueda, and M. Hada, *Chem. Phys. Letters* **250** (1996) 379.
114. K. Toyota, J. Hasegawa, and H. Nakatsuji, *Chem. Phys. Letters* **250** (1996) 437.
115. H. Nakatsuji, Y. Tokita, J. Hasegawa, and M. Hada, *Chem. Phys. Letters* (1996) in press.
116. K. Toyota, J. Hasegawa, and H. Nakatsuji, *J. Phys. Chem.* submitted.
117. H. Nakai, H. Morita, and H. Nakatsuji, *J. Phys. Chem.* (1996) in press;
H. Morita, H. Nakai, P. Tomasello, and H. Nakatsuji, *Bull. Chem. Soc. Jap.* (1996)

in press.
118. C. C. Ballard, M. Hada, and H. Nakatsuji, *Bull. Chem. Soc. Jap.* (1996) in press.
119. V. Galasso, *Chem. Phys.* (1996) in press.
120. H. Nakatsuji, *J. Chem. Phys.* **87** (1987) 4995.
121. H. Nakatsuji, H. Nakai, and Y. Fukunishi, *J. Chem. Phys.* **95** (1991) 640.
122. D. J. Rowe, *Rev. Mod. Phys.* **40**, 153 (1968).
123. T. Shibuya and V. Mckoy, *Phys. Rev.* **A2** 2208 (1970).
124. J. Rose, T. Shibuya, and V. Mckoy, *J. Chem. Phys.* **58** (1973) 74.
125. D. Yeager, V. McKoy and G.A. Segal, *J. Chem. Phys.* **61** (1974) 755.
126. H. Koch and P. Jørgensen, *J. Chem. Phys.* **93** (1990) 3333.
127. H. Koch, H. J. A. Jensen, P. Jørgensen, and T. Helgaker, *ibid.* **93** (1990) 3345.
128. D. Mukherjee and P. K. Mukherjee, *Chem. Phys.* **39** (1979) 325;
S. Adnan, S. Bhattacharya, and D. Mukherjee, *Mol. Phys.* **39** (1980) 519.
129. J. Geertsen, M. Rittby, and R. J. Bartlett, *Chem. Phys. Letters* **164** (1989) 57;
D. C. Cmomeau and R. J. Bartlett, *ibid.* **207** (1993) 414.
130. J. F. Stanton and R. J. Bartlett, *J. Chem. Phys.* **98** (1993) 7029.
131. J.F. Stanton and J. Gauss, *J. Chem. Phys.* **101** (1994) 8938.
132. M. Nooijen and R. J. Bartlett, *J. Chem. Phys.* **102** (1995) 3629.
133. D. J. Wadt and R. J. Bartlett, *J. Chem. Phys.* **101** (1994) 3073.
134. J. P. Jasinski, S. L. Holt, J. H. Wood, and L. B. Asprey, *J. Chem. Phys.* **63** (1975) 757.
135. R. M. Miller, D. S. Tinti, and D. A. Case, *Inorg. Chem.* **28** (1989) 2738.
136. J. Fernandez, G. Lespes, A. Dargelos, *Chem. Phys.* **111** (1986) 97.
137. G. Moe, A. C. Tam, and W. Happer, *Phys. Rev.* **A14** (1976) 349.
138. W. R. Wadt and P. J. Hay, *J. Chem. Phys.* **82** (1985) 284.
139. S. R. Langhoff, C. W. Bauschlicher and H. Partrige, *J. Phys.* **B18** (1985) 13.
140. S. Huzinaga, J. Andzelm, M. Klobukowski, E. Radzio-Andzelm, Y. Sakai and H. Tatewaki, *Gaussian basis sets for molecular calculations* (Elsevier, Amsterdam, 1984).
141. W. C. Ermler, Y. S. Lee, K. S. Pitzer, and N. W. Winter, *J. Chem. Phys.* **69** (1971) 716.
142. S. Y. Chen and M. Takeo, *Rev. Mod. Phys.* **29** (1957) 20.
143. M. Gouterman, *The porphyrins*, edited by D.Dolphin, (Academic, NewYork, 1977), Vol. 3.
144. L. Edwards and D. H. Dolphin, *J. Mol. Spectrosc.* **38** (1971) 16.
145. U. Nagashima, T. Takada, and K. Ohno, *J. Chem. Phys.* **85** (1986) 4524.
146. J. B. Foresman, M. Head-Gordon, J. A. Pople, and M. J. Frisch, *J. Phys. Chem.* **96** (1992) 135.
147. Y. Yamamoto, T. Noro, and K. Ohno, *Int. J. Quantum Chem.* **42** (1992) 1563.
148. M. Merchán, E. Ortí, and B. O. Roos, *Chem. Phys. Letters* **226** (1994) 27.
149. J. W. Weigl, *J. Mol. Spectrosc.* **1** (1953) 133.
150. B. G. Anex and R. S. Umans, *J. Am. Chem. Soc.* **86** (1964) 5026.
151. B. O. Roos, K. Andersson, and M. P. Fülscher, *Chem. Phys. Letters* **192** (1992) 5.

152. L. Serrano-Andrés, M. Merchán, I. Nebot-Gil, B. O. Roos, and M. P. Fülscher, *J. Am. Chem. Soc.* **115** (1993) 6184.
153. M. P. Fülscher, K. Andersson, and B. O. Roos, *J. Phys. Chem.* **96** (1992) 9204.
154. R. J. Cave and E. R. Davidson, *J. Phys. Chem.* **91** (1987) 4481.
155. J. M. O. Matos, B. O. Roos, and P. Malmqvist, *J. Chem. Phys.* **86** (1987) 1458.
156. M. H. Palmer and I. C. Walker, *Chem. Phys.* **133** (1989) 113.
157. H. Sekino and H. Kobayashi, *J. Chem. Phys.* **75** (1981) 3477.
158. J. D. Baker and M. C. Zerner, *Chem. Phys. Letters* **175** (1990) 192.
159. R. P. Linstead and M. Whally, *J. Chem. Soc.* (1952) 4839
160. S. S. Dvornikov, V. N. Knyukshto, V. A. Kuzmitsky, A. M. Shulga and K. N. Solovyov, *J. Lumin.* **23** (1981) 373
161. L. Edwards and M. Gouterman, *J. Mol. Spectry* **33** (1970) 292
162. S. Huzinaga, *J. Chem. Phys.* **42** (1965) 1293.
163. I. Morishima, Y. Takamuki, and Y. Shiro, *J. Am. Chem. Soc.* **106** (1984) 7666.
164. Y. Tokita, K. Yamaguchi, Y. Watanabe, and I. Morishima, *Inorg. Chem.* **32** (1993) 329.
165. J. Fajer, D.C.Borg, A. Furman, D. Dolphin, and R.H. Felton, *J. Am. Chem. Soc.* **92** (1970) 3451.
166. M. Satoh, Y. Ohba, S. Yamaguchi, and M. Iwaizumi, *Ionrg. Chem.* **31** (1992) 298.
167. M. W. Makinen and W. A. Eaton, *Ann. N. Y. Acad. Sci.* **206** (1973) 210.
168. T. Iizuka, H. Yamamoto, M. Kotani, and T. Yonetani, *Biochim. Biophys. Acta* **371** (1974) 126.
169. R. H. Austin, K. W. Beeson, L. Eisenstein, H. Frauenfelder, and I. C. Gunsalus, *Biochemistry* **14** (1975) 5355.
170. N. Alberding, R. H. Austin, K. W. Beeson, S. S. Chan, L. Eisenstein, H. Frauenfelder, and T. M. Nordlund, *Science* **192** (1976) 1002.
171. T. Nakajima and H. Nakatsuji, to be submitted.
172. H. Nakatsuji, Prog. Surf. Sci., to be submitted.